Study on the impact of physical treatment on tumors and testicular tissues

Department of Pharmaceutical Health Chemistry

Graduate School of Pharmaceutical Sciences

Tokushima University, Japan

MAHRAN MOHAMED ABDELEMAM MAHRAN

2022

Study on the impact of physical treatment on tumors and testicular tissues

Ph.D. Thesis

Graduate School of Pharmaceutical Sciences

Tokushima University, Japan

By

MAHRAN MOHAMED ABDELEMAM MAHRAN

September 2022

List of contents

List of figures

Abbreviations

17 β-HSD: 17β-hydroxysteroid dehydrogenase
3 β-HSD: 3β-hydroxysteroid dehydrogenase
BAX: Bcl-2-associated X protein
BCL2: B-cell lymphoma 2
BSA: bovine serum albumin
cAMP: cyclic adenosine monophosphate
CatSper channel: cation channel of sperm
CatSper β: CatSperbeta
CatSper γ: CatSper gamma
CatSper δ: CatSper delta
CatSper ε: CatSper epsilon
CatSper ζ: CatSper zeta
cdk1: cyclin-dependent kinase 1
CLSM: confocal laser scanning microscope
Cx43: connexin 43
DAPI: 4',6-diaminidino-2-phenylindole
DiIC18: 1,1'-dioctadecyl-3,3,3',3'-tetramethylindocarbocyanine perchlorate
DMEM: Dulbecco's modified Eagle's medium
DOX-NP: PEG-modified doxorubicin (DOX) encapsulated nanoparticles
DSPE-PEG 2000: 1,2-distearoyl-sn-glycero-3-phosphoethanolamine-N-[amino(polyethylene glycol)-2000] (ammonium salt)
ECM: Extracellular matrix
EPC: Egg phosphatidylcholine
EPR: Enhanced permeability and retention
FDA: Food and Drug Administration
HEPES: N-2-hydroxyethylpiperazine-N'-2-ethanesulfonic acid
HMOX-1: haem oxygenase-1
HPLC: high performance liquid chromatography
Hsc70: heat shock cognate 70
HSF1:heat shock factor 1
Hsps: Heat shock proteins
Hv1:Voltage-gated H^+ channel
IL-10: Interleukin-10

IP: Iontophoresis
KSper: sperm-specific K^+ channel
LH: luteinising hormone
LHR: luteinising hormone receptor
NF-κB: Nuclear factor kappa B
NO: nitric oxide
NOS: nitric oxide synthase
OCT: optimal cutting temperature compound
PBS: phosphate-buffered saline
PKC: Protein Kinase C
PVDF: polyvinylidene difluoride
RNS: reactive nitrogen species
ROS: reactive oxygen species
sACY: soluble adenylyl cyclase
SDS-PAGE: sodium dodecyl sulfate–polyacrylamide gel electrophoresis
StAR: steroidogenic acute regulatory protein
TNF: Tumour Necrosis Factor
WEC: weak electric current
ZP: zona pellucida

Abstract

Abstract

Although, using physical stimuli is accepted in the area of oncology, it may be harmful to normal tissue. So this study was conducted to investigate the effects of two different physical treatments (weak electric current (WEC) and hyperthermia) on tumor and testicular tissues, respectively. In the first section of this thesis, I investigated the effects of WEC on tumor. I postulated that WEC amplifies the enhanced permeability and retention (EPR) effect in solid tumors by dissociating intercellular junctions based on a previous study that reported that WEC triggers an intracellular signaling pathway in the skin, which opens the intercellular space apparatus. Based on this premise, I tested the antitumor activity of WEC treatment in combination with PEG-modified doxorubicin encapsulated nanoparticles (DOX-NP) or alone in B16-F1 melanoma bearing mice. I found that WEC treatment enhanced the EPR effect of DOX-NP. Also, WEC treatment alone prevented tumor growth. To clarify the mechanism of the tumor growth prevention effect of WEC, I examined the effect of WEC treatment on B16-F1 melanoma cells in vitro. I found that WEC treatment prevented the proliferation, but no cytotoxic effect was observed. Furthermore, WEC treatment suppressed cyclin B1 protein expression, which is considered a key regulatory protein involved in mitosis. In the second section of this thesis, I evaluated the impact of thermal treatment on testicular cells. Previous researchers have found that hyperthermia impairs testicular function through a variety of mechanisms, including apoptosis, oxidative stress, and induction of heat shock proteins, but the exact mechanism is unknown. Here, I studied the effect of thermal treatment on male fertility, focusing on the CatSper channel (cation channel of sperm) as a new mechanism of hyperthermia-induced testicular injury and examined the time dependent change of this cation channel after heat treatment. I found that thermal treatment caused notable downregulation of CatSper1 and-2 gene expression on day 1, day 14 and day 35. I also found a reduction in testis weight and a deterioration of sperm motility in heat stressed rats, which was correlated with reduced CatSper gene expression and the decline of this gene expression was dependent on the incubation time after heat treatment and not the repetition of heat exposure. In conclusion, physical treatment by

WEC and heat reduced the tumor and testis size, respectively, by two distinct mechanisms.

General introduction

General introduction

Physical treatments like iontophoresis (IP), hyperthermia, irradiation, and ultrasound are commonly used these days. There are several applications of these treatments. IP is a transdermal technology that uses WEC (weak electric current) to administer medications like lidocaine and dexamethasone **[1]** and is used to treat palmar and plantar hyperhidrosis **[2]**. Whole-body hyperthermia can be utilized to cure metastatic cancer cells that have spread rapidly inside the body **[3]**. Irradiation is also a curative therapy for many cancers, as well as an effective palliative treatment for individuals suffering from tumor-related symptoms **[4]**. The FDA has approved the use of therauptic ultrasound for the treatment of uterine fibroids **[5]**, cardiac ablation **[6]**, and visceral soft tissue ablation **[7]**.

However, it has been reported that the applications of hyperthermia, ultrasound, and irradiation affect normal tissue such as the testis. Rat testis showed an increased rate of germ cell apoptosis following hyperthermia **[8]** or irradiation **[9]**. Also, using therapeutic ultrasound resulted in impaired spermatogenesis in rats **[10]**. In this part of the thesis, I focused on the physical treatments by WEC and heat in relation to tumor growth and testis function, respectively.

1. IP

IP is a non-invasive method that uses physiologically acceptable electric current to facilitate and enhance transdermal delivery of various drugs into the body **[11]**.

1.1. IP mechanisms

IP increases drug flow through the skin through three mechanisms: electrorepulsion, electoroosmosis **[12]**, and damage effect from current-induced skin permeation **[13]**. Electrorepulsion occurs when molecules are placed under under an electrode with a similar charge. It increases the flux of small lipophilic cations **[14]**.Whenever an electric potential difference across a membrane occurs, electroosmotic flow occurs. This flow is always in the same direction as that of counterions. Due to the negatively charged

nature of human skin, the electroosmotic flow is from anode to cathode. As a result, cathodic delivery of anions is hampered, while electrosmosis aids anodic transport of cations. Electroosmosis involves the delivery of both neutral and positively charged ions **[15]**.

1.2. IP pathway

There are three possible pathways for IP; the paracellular or intercellular ones, which occur between corneocytes along the lamellar lipids; the intracellular or transcellular ones that take place via the cells; and the shunt or appendageal pathways, which occur through sweat ducts, hair follicles, and secretary glands **[16]**. Shunt pathways are preferred by ions. Hydrophilic molecules are more likely to be found in hair follicles, whereas hydrophobic molecules are more likely to be found in the lipid intercellular parts of epidermal keratinocytes and stratum corneum lipid membranes **[17]**.

1.3. Advantages of IP

IP has several benefits, including the avoidance of the hepatic first-path effect; The risk of overdosing or underdosing can be eliminated through the delivery of drugs at the required therapeutic dose; prevention of absorption variation **[18]**; improved patient compliance **[19]**; a significant reduction in intra- and inter-subject variance in drug delivery **[20]**; and reduced needle insertion pain **[21]**.

1.4. Factors affecting IP

IP drug delivery is affected by numerous factors, which include the physicochemical properties of the molecules (charge, molecular size, polarity, and concentration), as well as the drug formulation (pH, ionic strength, presence of co-ions), and used current (strength, duration, constant vs. pulsed current).

1.4.1. Molecular size

The drug's molecular size has an impact on its iontophoretic transport capability. The permeability coefficient reduces as the molecule size increases, as ions that are small transfer faster than those that are larger **[22]**.

1.4.2. Charge

Although cations have been demonstrated to transport better than anions, this is not so straightforward because an increase in charge requires a fall in pH, which reduces the electrotransport process and causes the drug to bind strongly to the membrane, forming a reservoir that slows the rate at which the steady state flow is reached **[23]**.

1.4.3. Concentration

The apparent steady state flux of a number of medicines, including as rotigotine and ketorolac, has been demonstrated to rise as concentration increases **[24]**.

1.4.5. Polarity

In general, hydrophilic compounds are considered ideal candidates for optimum flux; for example, the flow of nalbuphine and its ester improved when the lipophilicity of the compound dropped **[25]**.

1.4.6. pH

pH affects the iontophoretic delivery of drugs in two important ways **[26]**. First, increasing the skin pH above 4 helps in ionization of the carboxylic acid moieties and the anodal IP enhances cationic drug permeation. Second, drug ionization is affected by donor solution pH as weakly basic drugs will be ionized to a lesser degree at pH higher than their pKa and will permeate through electro-osmosis rather than electromigration **[19]**.

1.4.7. Ionic strength

Iontophoretic permeation of pharmaceuticals is directly connected to the ionic strength of a drug delivery system **[27]**. Drugs like ketorolac exhibited greater flux when ionic strength decreased **[24]**.

1.4.8. Presence of co-ions

When a co-ion (an ion with the same charge as the drug) is present, competition between the drug and the co-ion occurs, resulting in a reduction

in the proportion of current carried by the drug and, as a result, a reduction in drug transdermal flux **[28]**.

1.4.9. Current strength

Theoretically, there is a direct relationship between the flux of drug molecules and current intensity. To avoid patient discomfort, non-specific vascular reactions, and skin irritation, the current needs to be limited to 1mA/cm^2 area **[29]**.

1.4.10. Current duration

With increasing application time, the drug's iontophoretic penetration rose linearly. For instance, with an increasing duration of iontophoretic application of insulin, blood glucose levels were reduced by 2-4 folds **[30]**.

1.4.11. Constant vs. pulsed current

Continuous current causes skin polarization, which reduces the efficacy of iontophoretic administration. Pulsed current can be used to solve this issue. When compared to continuous current, pulsed current improved the iontophoretic transport of peptides and proteins **[31]**.

1.5. Delivery of macromolecules by IP

To know how IP permeates drugs through the skin barrier, Hama et al. applied IP with cationic liposome through rat skin. Hama et al. showed that WEC triggers an intracellular signaling pathway in the skin, which opens the intercellular space apparatus, which allows the migration of liposomes through the skin barrier. Two of these processes are cleavage of gap junctions via lowering connexin 43 levels and depolymerization of F-actin associated with tight junctions **[32]**. Hasan et al. also reported that endocytosis is responsible for the low electric current-induced cellular uptake of siRNA **[33]**.

Although hydrophilic, charged, and low molecular weight molecules are the optimal candidates for IP, many scientists have been successful in delivering macromolecules. Kigasawa K. et al. investigated IP delivery of unencapsulated siRNA through skin and used IP of siRNA against IL-10 on

actopic dermatitis skin, discovering that IP significantly reduced IL-10 mRNA expression by 73% **[34]**. In B16-F1 melanoma-bearing mice, IP-mediated skin administration of CpG-ODN produced an immunological response and inhibited tumor growth **[35]**. Fukuta et al. revealed that in an imiquimod-induced psoriasis skin model, frequent administration of the anti-TNF drug etanercept (recombinant human soluble TNF-receptor: Fc fusion protein) by IP reduced IL-6 mRNA expression by 50% **[36]**. This author also found that a single dose of NF-B decoy ODN given by a combination of IP and the AT1002 analog peptide showed improved therapeutic advantages against psoriasis, decreasing epidermal hyperplasia as well as TNF-and IL-6 mRNA production **[37]**.

2. Physical treatment by heat

Male reproductive problems are increasing and becoming a major public health concern nowadays **[38]**. Infertility affects approximately 10-15% of all couples **[39]**, with male-related factors accounting for 50% of fertility problems **[40]**. Male reproductive dysfunction is associated with several factors, including psychological stress, obesity, smoking, prolonged exposure to hazardous toxic agents (chemotherapy, heavy metals, pesticide residues), chronic disorders like cancer and diabetes, and exposure to high temperatures **[41]**. These factors, individually or in combination, may have an influence on sperm production, ultimately leading to male infertility **[42]**.

2.1. Thermal regulation of testis

Normal spermatogenesis requires a temperature difference of 2 to 6 degrees Celsius between the male gonads and the body core in most mammals **[43]**. The scrotal temperature is kept below the body's normal body temperature by five anatomical factors. The first is the dartos muscle, a smooth muscle surrounding the scrotum which relaxes as the ambient or core temperature rises **[44]**. The second is the cremaster muscle fibres, skeletal muscle fibers in the spermatic cord that control the distance between the testes and the body **[45]**. The third is the testicular artery, which receives blood from the abdominal aorta and transports it to the testis, passing through the pampiniform plexus of veins, which returns blood from the testis. This

configuration aids in controlling scrotal temperature by allowing an exchange of heat between the arteries and the surrounding veins **[46]**. The fourth is the scrotal skin's lack of subcutaneous fat, and this allows heat loss from the scrotum **[47]**. The final one is the abundant sweat glands on the skin of the scrotum **[48]**. Damaged spermatogenesis can arise from impaired thermoregulation in the testis, resulting in temporary or permanent infertility **[49]**.

2.2. Factors that contribute to heat stress

2.2.1. Lifestyle and behavioral factors

2.2.1.1. Clothing and posture

Walking lowers scrotal temperatures compared to sitting because scrotal movement improves circulation of air and thermal dispersion **[50]**. Testicular temperature rises when the testis is cradled between the thighs or when lying down with the scrotum resting on the thighs in cases of prolonged sitting. The use of tight underwear on a regular basis has been shown to lower sperm quality as it reduces the amount of space available for scrotal mobility and air movement. and consequently increases genital temperatures **[51]**.

2. Hot baths and sauna

Full-body immersion in a heated Jacuzzi, a warm bath, or whirlpool for 30 minutes or more, three times a week for three months or longer, produces hyperthermia, which negatively affects sperm production **[52]**.

2.2.1.2. Laptop use

Using a computer on the lap is harmful to sperm parameters because it is near to the genital region and resting, including one leg adjacent to the other for lengthy periods of time raises scrotal temperature **[53]**.

2.2.1.3. Obesity

Obese males have altered testicular thermoregulation as a result of lower physical activity and increased sitting times, as well as higher fat

accumulation in the abdominal, spermatic cord, suprapubic, and upper thigh areas, all of which lead to spermatogenesis suppression **[54]**.

2.2.1.4. Occupational factors

Certain jobs involve exposure to strong levels of heat, such as welders **[55]**, ceramic oven operators, and beakers **[56]**, and this negatively affects fertility. Also, increased scrotal temperatures are more common in occupational drivers and people who have long daily drives **[57]**.

2.3. Effect of heat stress on spermatogenesis

2.3.1. Spermatogenesis process

Spermatogenesis takes place in seminiferous tubules in which germ cells and sertoli cells reside. During spermatogenesis, somatic sertoli cells that surround the seminiferous tubules support and nourish germ cells. The interstitial tissue between the seminiferous tubules including lymphatic and blood vessels, macrophages and Leydig cells, which produce growth factors and testosterone. Tubules are surrounded by peritubular myoid cells, which provide structural support, growth factors, and assist with fluid and sperm passage across the tubule lumen **[58]**.

Briefly, diploid spermatogonia (2C cells) transform into preleptotene spermatocytes, which become 4C cells after multiple mitotic divisions. After that, the first meiotic division produces secondary spermatocytes with two copies of each gene (2C cells). The secondary spermatocytes produce haploid spermatids (1C cells) after the second meiotic division, which will develop into spermatozoa **[59]**.

The rapid rate of mitosis in germ cells increases their susceptibility to thermal stress **[60]**. Pachytene and diplotene spermatocytes, and also early round spermatids, are the germ cells most vulnerable to heat in both rats **[61]** and humans **[62]**.

2.3.2. Effect of hyperthermia on sperm characteristics

Testicular heat induces changes in sperm parameters in both fertile and infertile males **[63]**. It promotes spermatogenic arrest and atrophy of the

testicular germinal epithelial cells **[51]**, and this is linked to a considerable drop in sperm concentration **[64]** and sperm motility **[65]**, resulting in poor sperm quality. Also, it reduces the formation of sperm membrane-covering proteins, culminating in more sperm with defective morphology **[66]**. Men subjected to hyperthermia have been found to have lower sperm quality and sperm motility, as well as aberrant sperm **[67]**. Rao et al. found that there was a significant drop in sperm concentration and motility in human individuals exposed to scrotal warming in a 43 °C water bath for 30 minutes a day for 10 consecutive days **[68]**. Hamerezaee et al. also demonstrated that workers showed decreased semen quality after exposure to hyperthermia **[69]**. Gong et al. revealed that the percentage of progressive motility in boar sperm subjected to heat at 42°C for 6 hours was significantly lower than the control **[70]**. Furthermore, rats treated with thermal stress at 32°C for 2 h/day for 7 weeks had a notable decrease in sperm motility compared with control group **[71]**. Sperm counts in laboratory mice subjected to 36°C whole body heat for two days showed a reduction 21 days later **[72]**. Mice subjected to 42°C for 30 minutes had lower sperm numbers as early as 7-21 days after the exposure **[73]**.

2.4. Heat stress-related mechanisms

The testis exhibits a variety of mechanisms in response to heat stress, including heat-shock response, oxidative stress response, and apoptosis, through modulating the expression of many genes **[49]**.

2.4.1. Heat-shock response

HSPs are a broad group of molecular chaperones that are essential for cell survival and development. Based on its similar molecular masses, it can be split into two groups. The first category includes ATP-independent HSPs with a molecular mass of 8 to 28 kDa, such as ubiquitin, the -crystallins, HSPB1 (also known as HSP 25 in mice or HSP 27 in rats and humans), and a variety of others **[74]**. The second one is ATP-independent HSPs with a molecular mass of 40 to 105 kDa, such as the 70 and 90 kDa groups. The stress-inducible HSP 70 and the constitutively expressed heat shock cognate 70 (HSC70) make up the 70 kDa group. Inducible HSP 90 and constitutively

expressed HSP 90 are the two primary isoforms of the 90-kDa category. Due to the difficulty of isolating these isoforms, much research has resorted to examining co-purified aggregates including both categories of HSP 90, collectively referred to the entire as HSP 90 **[75]**.

The heat shock factor 1 (HSF1) protein, which governs the production of HSPs, is one of the most important elements in the Heat Shock response. HSPs are required for spermatocytes to mature into healthy mature spermatozoa because of their crucial role in maintaining proper protein assembly and transport and preserving the cell from environmental stress **[76]**. HSPs have been found on the surfaces of mouse, rat, bull, boar, and human sperm, and members of the HSP70 family tend to be prominent on the surface of sperm **[77]**. HSP 90 is found in the testes of mouse **[78]**, pig **[77]**, and rat **[79]**. Lee et al. have identified high levels of HSP90 transcripts in mouse meiotic prophase spermatogenic cells. Male mice lacking HSF1 produce 20% fewer sperm and more sperm with abnormal head morphology **[80]**. Pei et al. found that heat stressed rabbits showed significant elevations of HSP60, HSP90, and HSC70 after a 9-week heat treatment **[81]**. Also, primary HSP70 mRNA and protein, as well as HSP90 mRNA, were upregulated in primary hepatocytes of broiler embryos subjected to heat stress **[82]**.

2.4.2. Oxidative stress response

ROS and RNS are powerful reactive chemicals that can be free radicals such as superoxide, peroxyl, hydroxyl, hydroperoxyl, nitrogen dioxide, and NO, or non-radicals such as hydrogen peroxide, hydrochlorous acid, nitrous oxide, peroxynitrite, and alkyl peroxynitrates. The oxidases and mitochondrial function pathways produce superoxide, whereas the Nitric Oxide Synthase (NOS) pathway generates NO **[83]**. ROS participates in all spermatozoal processes like acrosome reaction, capacitation, hyperactivation, and sperm-oocyte fusion **[84]**. In spite of this, excess ROS can harm sperm and result in infertility in men. Spermatozoa are extremely vulnerable to ROS-induced oxidation because sperm plasma membranes comprise high levels of polyunsaturated fatty acids such as docosahexaenoic acid, which has six double bonds per molecule **[85]**.

Hyperthermia has also been shown to have a negative impact on cell physiology by interrupting transcription and changing oxidative metabolism in animal and human tissues **[86]**. It promotes oxidative damage to the, leydig cells, germ cells, and sertoli cells in the testes **[87]**. It also affects oxidative stress markers like glutathione, a non-enzymatic antioxidant, as well as antioxidant enzymes like catalase and superoxide dismutase **[84]**.

Previous studies in rodents and primates showed that testicular heat stress (43 °C for 15 minutes) causes an increase in germ cell death via oxidative insult **[88]**. Delkhosh et al. demonstrated that Superoxide dismutase, glutathione peroxidase, and catalase activity were reduced in rat testis submerged in a water bath at 43°C for 20 minutes every other day for 8 weeks, but lipid peroxidation was increased **[89]**. In contrast, mice exposed to a single scrotal hyperthermia at 42°C for 30 minutes demonstrated increased mRNA expression of haem oxygenase-1 (HMOX-1) as well as glutathione peroxidase activity and ROS **[90]**.

2.4.3. Apoptosis response

Apoptosis occurs in the testis by means of two pathways: the intrinsic and extrinsic pathways **[91]**. The intrinsic pathway (or mitochondrial pathway) involves translocation of BAX from the cytosol to the mitochondria, where it stimulates cytochrome C release. When cytochrome C attaches to the apoptotic activating factor-1, the initiator caspase 9 is activated, followed by the executioner caspases 3, 6, and 7, culminating in apoptosis **[92]**. Members of the BCL2 protein family are implicated in this pathway by forming dimers with BAX **[93]**. The extrinsic pathway (also known as the death receptor pathway) includes Fas ligand activation of FAS protein on target cells, which triggers initiator caspase 8 and then executioner caspases, inducing apoptosis **[94]**.

Previous investigations suggested that heat promote germ cell apoptosis and DNA damage **[95]**. Kanter et al. reported that there was an increase in germ cell apoptosis on days 1 and 14, but a decrease on day 35 in rat testes heated to 43°C for 30 minutes **[8]**. Caspases-3 expression increased 9 fold or 27 fold in mice testes 6 h and 24 h after being exposed to 43°C for 30 minutes

[49]. The number of TUNEL-positive apoptotic cells in a mouse testis heated to 42°C for 15 minutes increased significantly after 12 hours of heat treatment **[96]**. Apoptosis may be time-temperature dependent **[97]**. Germ cell apoptosis is induced as early as 8 hours after local scrotal heat stress of 43°C for 20 minutes, while it was unaffected by lower temperatures of 39–40°C **[98]**.

2.5. Heat stress and testosterone synthesis

Testosterone synthesis is required for proper spermatogenesis **[99]**. Testosterone synthesis is activated by luteinising hormone (LH) in Leydig cells. Briefly, binding of LH to its receptors stimulates adenylyl cyclase, which boosts cyclic adenosine monophosphate (cAMP) generation in Leydig cells, and the latter activates multiple members of the steroidogenic pathway, resulting in enhanced testosterone synthesis **[100]**. Testosterone synthesis starts in the inner mitochondrial membrane by the enzymatical conversion of cholesterol. First, cholesterol must be transported from the cytoplasm to the inner membrane of the mitochondria by steroidogenic acute regulatory protein (StAR) **[101]**. After that, Cholesterol is transformed to pregnenolone under the action of the C27 cholesterol side-chain cleavage cytochrome P450 enzyme (CYP11A1) found in the inner mitochondrial membrane matrix. Pregnenolone then is converted into testosterone by 17α-hydroxylase/17,20 lyase (CYP17A1), 3β-hydroxysteroid dehydrogenase (3 β-HSD; HSD3B), and type 3 17β-hydroxysteroid dehydrogenase (17 β-HSD3, HSD17B) in the smooth endoplasmic reticulum **[102]**.

Testosterone is primarily produced in the Leydig cells and is essential for normal spermatogenesis. The synthesis of testosterone is severely harmed by heat stress in the testes **[103]**. Previous research revealed that rams exposed to scrotal insulation for 72 hours had lower serum levels of testosterone **[104]**, and serum testosterone concentrations were considerably lower in rats subjected to 43 °C for 30 minutes for 3, 5, or 10 days **[105]**. Li et al. revealed that adult rats subjected to a single hyperthermia at 43°C for 30 min exhibited low expression of cytochrome P450 family 17 (CYP17) and steroidogenic acute regulatory (STAR) protein in Leydig cells **[105]**. Yon et al. found that mouse testis heated at 43°C for 20 min exhibited a

considerable reduction in serological testosterone levels and testicular 3 β-HSD mRNA expression **[106]**.

2.6. CatSper channel and male fertility

2.6.1. Structure of the Catsper channel complex

On the plasma membrane of sperm, there are two types of sperm-specific ion channels: the Ca^{2+}-permeable CatSper (sperm cation channel) and the K^{+}-permeable KSper (sperm pH-regulated K^{+} channel), both of which are vital in fertilization **[107]**.

CatSper is a sperm-specific, weakly voltage-dependent, Ca^{2+}-selective, pH-sensitive ion channel that regulates the entry of positively charged calcium ions into sperm cells, which is required for sperm hyperactivation and male fertility **[108]**. It was identified in mouse sperm as a putative Ca^{2+} channel in 2001**[109]**.

The mammalian CatSper channel complex includes at least 10 different proteins, four pore-forming subunits (CatSper 1-4) and six accessory subunits (CatSper β, γ, δ, ε, ζ, and EFCAB9) **[110]**.

Each of CatSper's four pore-forming subunits has six transmembrane segments (S1–S6), each with two functionally distinct modules: the voltage sensor domain (S1–S4) and the pore-forming domain (S1–S6) (S1-P loop-S6). The fourth transmembrane segment (S4) contains many positively charged amino acid residues (lysine/arginine). Six positively charged amino acid (lysine or arginine) residues are found in CatSper-1. CatSper-2 includes four of these residues, but CatSper-3 and CatSper-4 only have two **[109]**. The degree of interspecies homology among mouse and human CatSper subunits is weak, varying from 50 % (CatSper-1) to 69 % (CatSper-4) **[111]**.

CatSper β has two transmembrane segments, also with two small cytoplasmic domains and a big extracellular domain **[112]**. A single transmembrane segment with a large extracellular domain and a short cytoplasmic tail makes up CatSper γ **[113]**. The CatSper δ gene was recently identified and has also a single transmembrane segment with a large extracellular domain and a short cytoplasmic tail **[114]**.

EF-hand calcium-binding domain-containing protein 9 or EFCAB9 is a new CatSper complex component and CatSper ζ direct binding partner. The EFCAB9-CatSper ζ complex binds specifically to the channel pore and provides pH-dependent activation and Ca^{2+} sensitivity, regulating the opening and closing of the CatSper channel **[110]**.

2.6.2. Localization the Catsper channel complex

According to the localization pattern in mice and humans, The CatSper channel is confined to the sperm principal piece **[115]**. CatSper1–3 is only found in the testis, whereas Catsper-4 is mostly found in the testis, with some faint amount in the lung and placenta tissues **[116]**.

The mouse CatSper-1 gene, located on chromosome 19, encodes a 686 amino acid protein, while the CatSper-2 gene, found on chromosome 2, encodes a 588 amino acid protein. CatSper-3, which is found on mouse chromosome 13, encodes a 395-amino-acid protein, while CatSper-4, which is found on mouse chromosome 4, encodes a 442-amino-acid protein **[117]**.

CatSper-1 **[109]**, CatSper-3, and CatSper-4 transcripts **[118]** are found in late-stage germ line cells (spermatids), whereas CatSper-2 is found in the early stages of spermatogenesis (pachytene spermatocytes) **[119]**. CatSper β **[112]**, CatSper γ **[113]**, and CatSper δ **[114]** are expressed in spermatocyte and spermatids of testes.

2.6.3. Calcium Homeostasis in Spermatozoa

Ion channels like voltage-gated H^+ channel (Hv1) and ion pumps like Na^+/Ca^{2+} exchanger, plasma membrane Ca^{2+} adenosine triphosphatase (ATPase), and sperm Na^+/H^+ exchanger have been proposed to work in tandem with the CatSper complex to maintain calcium homeostasis in sperm.

The Catsper channel is in charge of delivering transferring Ca^{2+} into the spermospore, which enhances sperm motility. The Ca^{2+}ATPase is a Ca^{2+}/H^+ exchanger that allows H^+ to enter the sperm cell while removing intracellular Ca^{2+} **[120]**. Moreover, the Na^+/Ca^{2+} exchanger exports one Ca^{2+} ion from sperm while allowing three Na^+ ions to enter, which is necessary to maintain

the intracellular Ca^{2+} equilibrium **[121]**. Hv1 is responsible for maintaining sperm intracellular pH **[122]**. KSper/SLO3 is a seven-transmembrane helical pH-sensitive channel that hyperpolarizes mouse spermatozoa, and this process promotes Ca^{2+} entry through CatSper channels. In male mice lacking SLO3, sperm motility is drastically reduced, resulting in sterility **[123]**. The sperm Na^{+}/H^{+} exchanger stimulates soluble adenylyl cyclase (sACY), which enhances CatSper-dependent Ca^{2+} entry through PKA-dependent phosphorylation **[124]**.

2.6.4. Role of the Catsper channel complex in male fertility

The CatSper channel, in conjunction with other ion channels and pumps, promotes calcium influx, which is required for large alterations in sperm motility which allows spermatozoa to travel through the female reproductive tract and contact the egg for fertilization **[125]**.

All four CatSper genes have a role in male fertility. CatSper-1 and CatSper-2 are currently considered vital for sperm flagella beat and hyperactivated sperm motility **[126]**, whereas CatSper-3 and CatSper-4 are involved in the acrosome reaction and egg coat penetration. Increase calcium influx initiates hyperactive motility. It is characterized by high amplitude whip-like asymmetrical tail bending that is non-progressive in aqueous low-viscosity conditions but progressive in the physiological viscosity of the upper female reproductive canal **[127]**.

Also, an increase in Ca^{2+} stimulates the acrosome reaction, which permits sperm to pierce the cumulus oophorus and the zona pellucida (ZP) enveloping the oocyte by releasing proteolytic enzymes. This response is essential for spermatozoa to effectively fertilize the egg **[128]**.

2.6.5. Physiological regulators of the Catsper channel complex

The complexity of the CatSper channel is crucial for its functional coordination, localisation to the flagella, and sensitivity to intracellular pH, progesterone, other proteins, and cell-signaling molecules and activators **[129]**.

There are some physiological stimuli that cause a CatSper dependent rise in Ca^{2+}, such as alkaline depolarization, ZP glycoproteins, and bovine serum albumin (BSA) **[130]**. The CatSper channel is activated by the alkaline environment of the female reproductive system **[131]**. Furthermore, progesterone and PGs promote Ca^{2+} influx in humans via activating CatSper directly **[130]**.

2.6.6. Factors impair CatSper channel complex

In both humans and animals, a disruption in the functionality of the CatSper channels and associated genes will cause fertility problems. Previous research has suggested that various factors influence the CatSper gene level in testicular tissue. Askari et al. found that in aged mice, overall CatSper gene expression and sperm motility decreased. However, by using Escanbil (Calligonum) extract, CatSper-2 and-4 gene expression and sperm motility improved **[132]**. Furthermore, Rezaian et al. investigated that lower CatSper-1 and-2 expression levels are hypothesized to be responsible for impaired sperm motility in the spinal cord injury animal model **[133]**. Also, Kerack may have an impact on the expression of CatSper genes **[134]**. It interferes with spermatogenesis by lowering sperm motility and CatSper expression levels.

Specifically disrupting CatSper 1–4 results in male infertility due to the impairment of channel function and hyperactivated motility **[135]**. It has also been demonstrated that CatSper-null mouse spermatozoa do not have the ability to fertilize ZP-intact oocytes **[109]**. Furthermore, CatSper δ null mice are infertile, and the level of CatSper-1 in spermatozoa is significantly reduced, implying that the CatSper δ subunit is required for the creation of a functional CatSper channel. In contrast to CatSper knockout mice, the absence of CatSper ζ disturbs the quadrilateral longitudinal nanodomain structure of the CatSper complex, while the channel is still functional, resulting in subfertility only in mutant animals **[114]**.

The objective of this study was to investigate the influence of physical treatment by WEC on tumor microenvironment and physical treatment by heat on testicular tissue.

Chapter I

Effect of weak electric current on tumor environment and growth

1.1 Introduction

The microenvironment of solid tumors is characterized by a leaky and loosely compacted vasculature with poor lymphatic drainage. Intravenously administered nano-sized agents, such as liposomes, micelles, polymeric conjugates, macromolecular drugs, and imaging agents, preferentially enter the interstitial space of tumors through leaky blood vessels and are retained there. This phenomenon is EPR effect **[136]**. Currently, the passive targeting of tumor using nanoparticles via EPR effect is the major strategy for anticancer therapy.

The therapeutic efficacy of nanoparticles encapsulating chemotherapeutic agents following passive targeting is hampered because of the significant heterogeneity of the EPR effect **[137]**. Tumors exhibit a variety of shapes, sizes, cell densities, microenvironments, and developmental stages. Their variable endothelial gaps, irregular blood flows, differences of stromal content, and distinct interstitial fluid pressures result in a non-uniform EPR effect **[138,139]**. For example, renal cell carcinoma, and hepatocellular carcinomas tend to have good vasculature networks that support a strong EPR effect **[140]**. In contrast, melanomas, pancreatic cancers, prostate cancers, and metastatic liver cancers are hypovascularized; the consequently poor EPR effect results in the suboptimal delivery of nanoparticles into these tumors **[141,142]**.

To ameliorate the delivery efficiency of nanoparticles, several approaches for the augmentation of the EPR effect have been evaluated. These strategies include increasing of tumor blood flow by either vasoconstriction or vasodilation **[143,144]**; modulation of the tumor vasculature by application of exogenous growth factors **[145]**; and changing of tumor stroma via enzymatic degradation of the extracellular matrix **[146]**. Although these strategies improved intratumor delivery and distribution of nanoparticles, the systemic administration of these pharmacological EPR modulators may also cause the delivery of NPs into the normal tissue.

To address the non-specific impacts of current EPR modulating strategies, effort to enhance the EPR effect locally within tumors have garnered

significant research attention. Several strategies reported in this regard include micro- or nanobubble assisted ultrasound, radiotherapy, and hyperthermia-based augmentation of nanoparticle EPR **[39,147,148]**. These strategies have achieved success to varying degree, but they all require very sophisticated instruments. Furthermore, the application of ionizing radiation and high intensity-ultrasound may damage the normal tissue surrounding a tumor **[149,150]**.

Here, I propose an alternative strategy, IP, for the enhancement of the EPR effect. IP is a noninvasive transdermal drug delivery technology that employs WEC treatment by placing electrodes on the skin surface **[20,33,151]**. A physiologically acceptable electric current density is used in WEC treatment does not exceed 0.5 mA/cm^2. It provides the driving force for the transdermal permeation of substances across the skin barriers **[180]**. Although small ionic and hydrophilic molecules are preferable for WEC based delivery, Kogure's group has successfully employed WEC in the noninvasive transdermal delivery of antibodies, siRNA, CpG oligo DNA, and NPs-encapsulated insulin **[34-36,153,154]**.

In pursuit of an understanding of the molecular mechanisms underlying WEC-mediated transdermal permeation of nanoparticles, Kogure's team observed that the application of WEC activates an intracellular signaling pathway leading to the opening of the intercellular space apparatus in the skin **[32,155]**. In particular, the WEC-mediated opening of gap junctions and depolymerization of F-actin associated with tight junctions dramatically altered cell-cell interactions and created a paracellular pathway that contributed to the transdermal permeation of macromolecules or nanoparticles **[32,152]**. Although the cutaneous physiology is different from that of tumors, in this study I hypothesized that the application of WEC on a solid tumor may increase the EPR effect via dissociation of intercellular junctions. Based on the hypothesis, I evaluated the EPR effect of PEG-modified DOX-NP, the status of gap junction expression in tumors, and the antitumor effect of DOX-NP co-administered with WEC. Taken together, this study offers a novel physical approach for the augmentation of the EPR effect and effective anticancer therapy by combination of nanoparticles and

WEC. In addition, I attempted to study the effect of WEC alone on tumor growth.

1.2 Materials and methods

1.2.1 Materials

I used C57BL/6J (5 weeks old, male) mice purchased from Japan SLC, Inc. (Shizuoka, Japan). All animal procedures in this study were conducted in compliance with Tokushima University Animal and Ethics Review Committee. B16-F1 murine melanoma cells (Dainippon Sumitomo Pharma Biomedical Co. Ltd., Osaka, Japan) were grown in 10% fetal bovine serum (FBS) supplemented Dulbecco's modified Eagle's medium (DMEM) and incubated at 37 °C in a 5% CO_2 atmosphere. Extracellular matrix (ECM) gel was obtained from Sigma-Aldrich Co., Ltd. (St. Louis, MO). 1,2-distearoyl-sn-glycero-3-phosphoethanolamine-N-[amino(polyethylene glycol)-2000] (ammonium salt) (DSPE-PEG 2000) and Egg phosphatidylcholine (EPC) were collected from NOF Corporation (Tokyo, Japan). The fluorescent compound 1,1'-dioctadecyl-3,3,3',3'-tetramethylindocarbocyanine perchlorate (DiIC18) was purchased from Thermo Fisher Scientific (Waltham, MA, USA). DOX, as doxorubicin hydrochloride, was obtained from Nacalai Tesque, Kyoto, Japan. An anti-connexin 43 (Cx43) antibody (mouse monoclonal) was purchased from Santa Cruz Biotechnology, Inc. (Santa Cruz, CA). An anti-Cx43 (phospho Ser367) antibody (rabbit polyclonal) was obtained from arigo Biolaboratories (Taiwan). A rabbit polyclonal anti- Protein Kinase C (PKC) (phospho T497) antibody, an Alexa Fluor 647 conjugated goat anti-mouse IgG antibody, and an Alexa Fluor 488 conjugated goat anti-rabbit IgG antibody were purchased from Abcam (Cambridge, UK).

1.2.2 Preparation of DOX-NP

DOX-NP was prepared according to our previous report **[156]**. In brief, EPC/DSPE-PEG2000 (10:1 molar ratio) was added in chloroform, and a thin lipid film was prepared by nitrogen gas drying. The resulting film was then

hydrated with 250 mM ammonium sulfate. For fluorescent labeling of the nanoparticles, DiIC18 (1 mol% of total lipid) was used. After incubation, a freeze-thawed cycle was performed three times using a dry ice/ethanol bath followed by extrusion through 100 nm pores of polycarbonate membrane filters (Nuclepore, Cambridge, MA, USA). After adjusting the size, the nanoparticle suspension was loaded into a PD-10 column (GE Healthcare Japan, Tokyo, Japan) and eluted with PBS to eliminate the excess ammonium sulfate. Then, ultracentrifugation of nanoparticles was carried out at 112500 g for 60 min at 4ºC followed by the addition of 20 mM HEPES (pH 8.8) to resuspend the nanoparticle pellet. The resulting nanoparticle suspension and a DOX solution (prepared at a concentration of 2 mg/ml in 20 mM HEPES (pH 8.8)) were then mixed together to incubate for 20 min at 37ºC. Next, the free DOX was separated by ultracentrifugation, and nanoparticle encapsulating DOX was evaluated by measuring the absorbance of DOX-NP dissolved in Triton X-100 (1%) at 484 nm. The nanoparticle size, ζ-potential, and polydispersity index were measured with a Zetasizer Nano ZS (Malvern Instruments, Worcestershire, UK). The average particle diameter was 140.83 ± 13.30, the ζ-potential was -1.64± 1.32 mV, and the polydispersity index was 0.23 ± 0.02.

1.2.3 Application of WEC and evaluation of DOX-NP accumulation in tumors

To develop melanoma-bearing mice, a suspension of 1×10^6 B16-F1 cells and ECM gel were mixed following a ratio of 5:1 (v/v), and the cells were implanted into the left posterior flank of mice that were 5 to 6 weeks of age **[157]**. After inoculation, tumor volumes were evaluated over time following this formula: tumor volume = $0.4 \times a \times b^2$ where the tumor volume is calculated in mm^3, *a* indicates the larger diameter in mm, b indicates the smaller diameter in mm. Intratumor accumulation of NPs following WEC application was evaluated when the tumor volume reached approximately 500 mm^3. Intravenous (IV) injection of DilC18-labeled DOX-NP was performed 1 h before the WEC treatment. For the application of WEC, anesthesia was induced in mice by intraperitoneal administration of chloral

hydrate (400 mg/kg) in phosphate-buffered saline (PBS), and the hair covering the tumor was trimmed. Ag-AgCl electrodes (3 M Health Care, Minneapolis, MN, USA) with a thin layer of PBS-soaked cotton on the adhesive surface was applied to the tumor surface. The tumor was then treated with a constant current (0.4 mA/cm^2 for 1 h) by adjusting the electrodes to an external power supply (model TCCR-3005, TTI ellebeau, Inc., Tokyo, Japan). After twenty-four hours of DOX-NP administration, tumors were collected and sized into appropriately pieces. The resulting tumor tissues were subjected to snap-frozen in optimal cutting temperature (OCT) compound in a dry-ice/ethanol bath and sectioned at 10 μm thickness with a cryostat. Next, tumor sections were stained with 4',6-diaminidino-2-phenylindole (DAPI) (Dojindo, Kumamoto, Japan) and mounted with PermaFluor Aqueous Mounting Medium (Thermo Fisher Scientific), followed by observation with an LSM700 confocal laser scanning microscope (CLSM) (Carl Zeiss, Germany). For quantitative analysis, the fluorescence intensity of tumor cross-sections was quantified using ImageJ software.

1.2.4 Determination the Effect of WEC on the pharmacokinetics (blood retention of DOX-NP) after administration of DOX-NP to normal mouse without cancer

IV injection of DOX-NP (3 mg DOX per Kg) was performed 1 h before the WEC treatment (0.4 mA/cm^2 for 1 h). WEC treatment was performed as described in the materials and methods. After 6, 12, 24 and 48 h, the blood was collected, and plasma was obtained. Then, the concentration of DOX was quantified by high performance liquid chromatography (HPLC). The mobile phase of HPLC consist of methanol and 20 mM ammonium acetate (50: 50 (v/v %)), the octa decyl silyl column (TSK gel ODS-80 TM (Tosoh, Japan)) was used, and DOX was detected by UV at 252 nm. The concentration of DOX in the plasma after deproteinization was calculated using calibration curve of DOX.

1.2.5 Immunohistochemical analysis of Cx43, phospho Cx43 (Ser367), and phospho PKC (T497) in tumor cross-sections after WEC treatment

Immediately after WEC treatment as described above, tumors were harvested and 10 μm frozen sections were generated using a cryostat. After washing with PBS (two times for 5 min) all tumor sections were blocked by PBS containing 3% bovine serum albumin (BSA) and Triton- X-100 (0.1%, 50 μl) for 1 h at room temperature. Then, three additional washing steps were performed with PBS for 2 min and cross-sections were incubated with mouse anti-Cx43, rabbit anti-Cx43 (phospho Ser367), or rabbit anti-PKC (phospho T497) in 3% BSA/PBS at dilutions recommended by the manufacturer. After overnight incubation at 4 °C, three washing steps were carried out with PBS for 2 min, and then cross-sections were treated with an Alexa Fluor 647 conjugated anti-mouse IgG antibody or an Alexa Fluor 488 conjugated anti-rabbit IgG antibody in 3% BSA/ PBS for 1 h at room temperature followed by manufacturer's instructions. Next, sections were subjected to wash again with PBS and then observed with CLSM. Fluorescence intensity of antibody staining was quantified using ImageJ software.

1.2.6 Investigation of the antitumor activity of DOX-NP in combination with WEC After inoculation with B16-F1 cells in mice

After inoculation with B16-F1 cells, mice (n=24) were randomly divided into four experimental groups as WEC (-) (untreated), WEC (+) (treated with WEC), DOX-NP (treated with DOX-NP), and DOX-NP + WEC (+) (treated with DOX-NP combined with WEC). IV administration of DOX-NP (3 mg DOX per Kg) was started when tumor volumes reached approximately 100 mm^3 and continued it on the scheduled days. After 1 h of DOX-NP administration, WEC (0.4 mA/cm^2 for 1 h) was applied on the tumor as described above. Over the study period, tumor volume and body weight were monitored. Mice were sacrificed at day 20 and tumors were harvested.

1.2.7 Cell culture

B16-F1 murine melanoma cells (Dainippon Sumitomo Pharma Biomedical Co. Ltd., Osaka, Japan) were grown in 10% fetal bovine serum (FBS) supplemented Dulbecco's modified Eagle's medium (DMEM) and incubated at 37 °C in a 5% CO_2 atmosphere.

1.2.8 WEC of cells

B16-F1 cells were cultivated at 1×10^5 cells per dish on 35 mm dishes. Ag-AgCl electrodes with a 2 cm^2 surface area (3 M Health Care, Minneapolis, MN, USA) were placed into the dish and cells were treated with a constant current of 0.34 mA cm^{-2} for 15 min at 24 h and 48 h after cultivation.

1.2.9 Determination of cell proliferation and viability of B16-F1 melanoma cells following WEC using trypan blue exclusion method

After 24 h of WEC, the cells were treated with trypsin and collected for measurement of cell viability using the trypan blue staining method. Cell viability is the percentage obtained by dividing the number of cells stained with trypan blue by the total number of cells.

1.2.10 Western blotting analysis of cyclin B1 protein after WEC treatment

Western blotting was performed according as follow. Briefly, 1×10^5 B16-F1 cells were seeded in 35 mm dishes. After 24 h of WEC, the cells were washed with PBS and treated with lysis buffer (25 mM Tris-HCl [pH 6.5], 1% [v/v] glycerol, 1% [v/v] SDS, 5% 2-mercaptoethanol and the phosphatase inhibitor cocktail PhosSTOP [Sigma Aldrich]). The amount of protein in the samples was determined by BSA Protein Assay (Thermo Fisher Scientific Inc., Waltham, MA, USA) and equal amounts of proteins (20 μg/lane) were loaded on 10% SDS-PAGE gels. Proteins were separated

by SDS-PAGE and transferred to polyvinylidene difluoride (PVDF) membranes that were then blocked by 5% skim milk in Tween solution (500 mM Pi buffer, 150 mM NaCl, 0.16% [v/v] Tween 20). Membranes were incubated with primary antibody (diluted and incubated according to the manufacturer's instructions) followed by incubation with the indicated secondary antibody diluted 1:3000. The blots were detected using ECL Western blotting detection reagent (GE Healthcare, Waukesha, WI) and a C-DiGit blot scanner (LI-COR Biosciences GmbH, Germany). Quantitative analysis of blots was performed by Image Studio Digits software (ver. 5) (LI-COR Biosciences GmbH, Germany). In this analysis, GAPDH was used as an internal control.

1.2.11 Statistical analysis

A one-way ANOVA followed by a Tukey *post-hoc* test was conducted for statistical analysis. Comparisons between two groups were accomplished by a Student's *t*-test. Data were representing as means ± standard deviations (SD). P values < 0.05 were considered to be significant.

1.3 Results

1.3.1 The effect of WEC on the intratumor accumulation of DOX-NP

I first examined the effect of WEC on the intratumor accumulation of DOX-NP. After IV administration of DiIC18-labeled DOX-NP into a tumor-bearing mouse, WEC was applied to the surface of the tumor. After indicated incubation time, tissue from the tumor was processed for frozen-sectioning, and then the nanoparticle accumulation into the tumor sections was observed by CLSM. From these observations, it was found that 24 h after WEC, the fluorescent signal was markedly increased in tumor tissue sections. In contrast, few fluorescent signals were observed in tissue from control tumors that did not receive WEC mentioned as WEC (-) (Fig. 1).

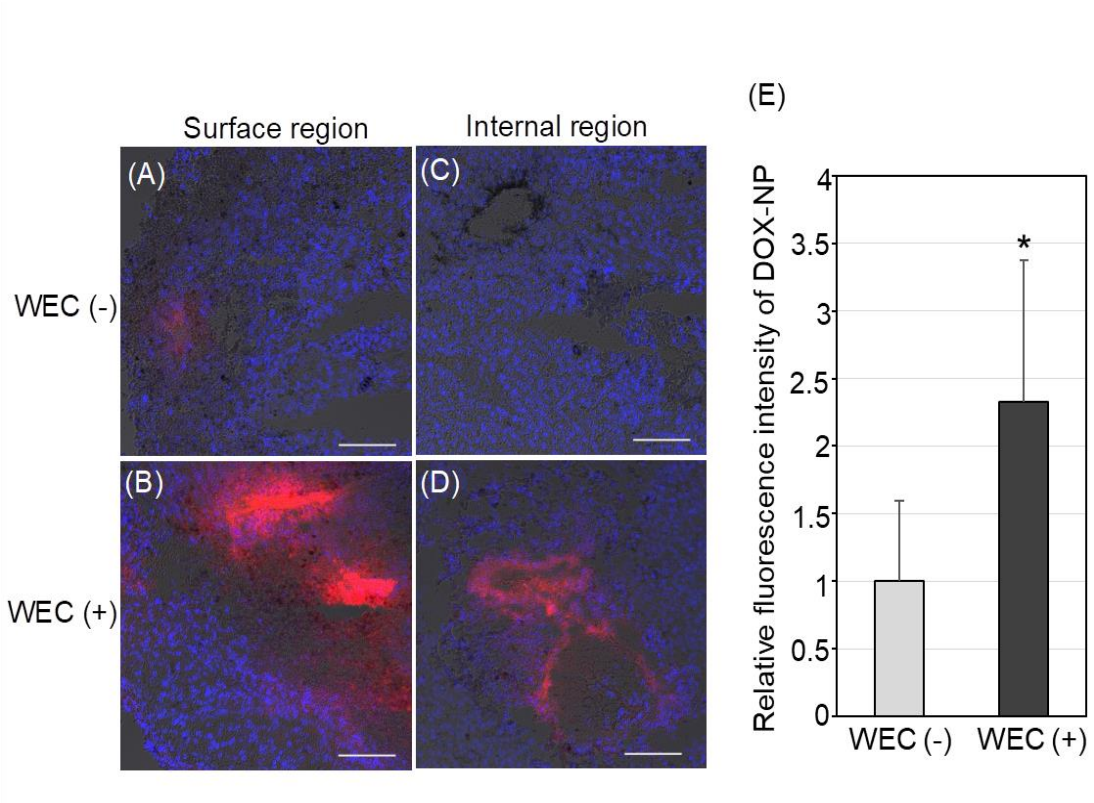

Fig.1 Effect of WEC on intratumor accumulation and distribution of DOX-NP. DilC18-labeled DOX-NP was administered into mice bearing B16-F1 tumors via an IV route following application of WEC on the surface of the tumor. After 24 h of WEC, tumors were collected, and their cross sections of various regions were examined with CLSM: (A) untreated surface region; (B) surface region subjected to WEC; (C) untreated internal region; (D) internal region

subjected to WEC. Red indicates the accumulation of DOX-NP while blue indicates DAPI-stained nuclei. Scale bars indicate 100 μm. (E) Quantitative analysis of DOX-NP accumulation increased by WEC. Relative fluorescence intensity of tumor sections was quantified by using image analysis software ImageJ. Data are expressed as mean ± S.D ($n > 3$). *$p < 0.05$.

1.3.2 Effect of WEC on the pharmacokinetics (blood retention of DOX-NP) after administration of DOX-NP to normal mouse without cancer

I also examined the effect of WEC on the pharmacokinetics (blood retention of DOX-NP) after administration of DOX-NP to normal mouse without cancer inoculation. In this experiment, I used normal mice, not tumor bearing mice, to avoid the change of pharmacokinetics of DOX-NP by enhancement of EPR effect by WEC. DOX concentrations in blood after intravenous injection of DOX-NP with or without WEC treatment were almost the same.

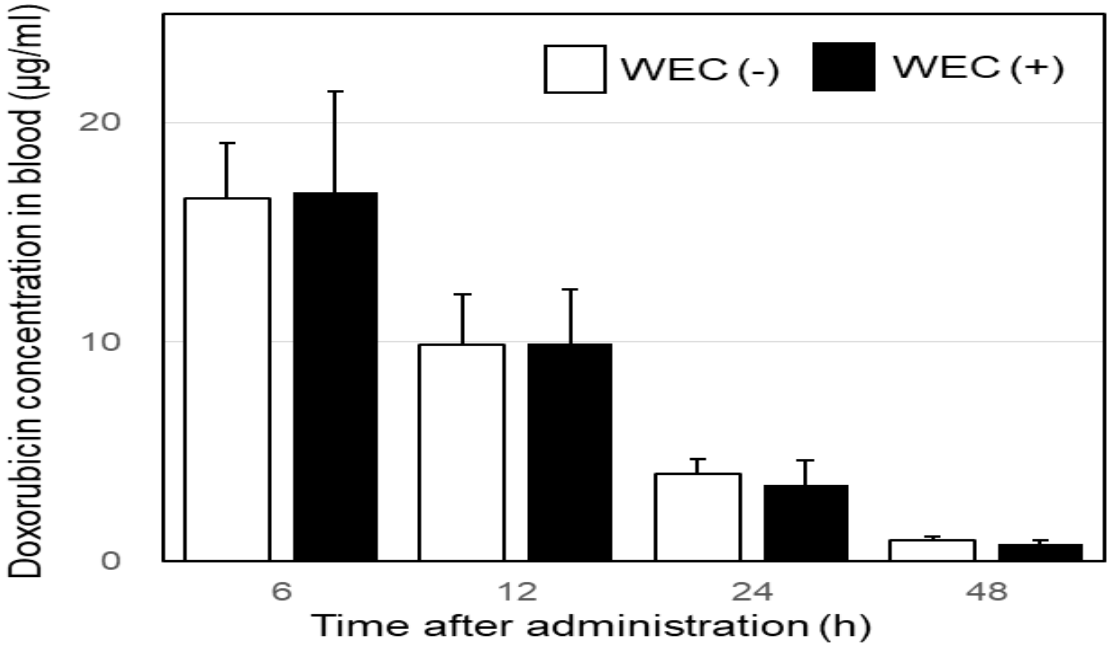

Fig. 2 Effect of WEC on doxorubicin concentration in blood after administration of DOX-NP to normal mouse without cancer inoculation. IV injection of DOX-NP (3 mg DOX per Kg) was performed 1 h before the WEC treatment (0.4

mA/cm^2 for 1 h). WEC treatment was performed as described in the MATERIALS AND METHODS. After 6, 12, 24 and 48 h, the blood was collected, and plasma was obtained. Then, the concentration of DOX was quantified by high performance liquid chromatography (HPLC). The mobile phase of HPLC consist of methanol and 20 mM ammonium acetate (50: 50 (v/v %)), the octa decyl silyl column (TSK gel ODS-80 TM (Tosoh, Japan)) was used, and DOX was detected by UV at 252 nm. The concentration of DOX in the plasma after deproteinization was calculated using calibration curve of DOX.

1.3.3 The expression levels of Cx43, phospho Cx43 (Ser367), and phospho PKC (T497) in tumors following WEC

Next, I evaluated the expression levels and phosphorylation of the gap junction protein Cx43 in tumors following WEC. Interestingly, I found that WEC treatment significantly reduced the amount of Cx43 by approximately 57% of control levels (Fig. 3) while it increased the amount of phosphorylated Cx43 by approximately 25% of control levels (Fig. 4). To further investigate gap junction formation following WEC, we examined the expression and phosphorylation of PKC. Here, I found that phosphorylation of PKC was upregulated in the tumor immediately after application of WEC (Fig. 5). Quantitatively, the amount of phosphorylated PKC was increased by approximately 28% of control levels in WEC-treated tumors.

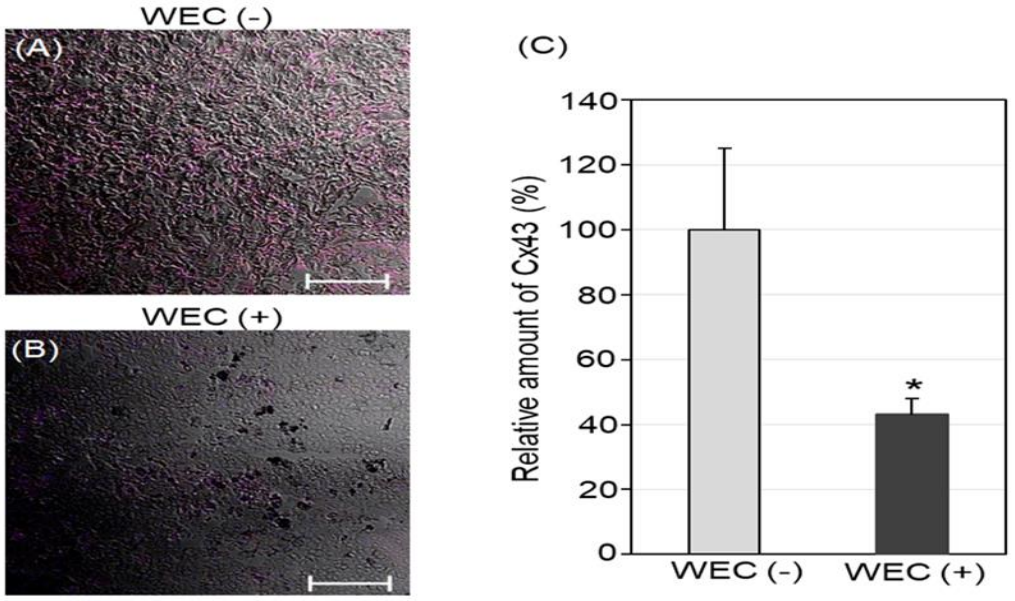

Fig. 3 Immunohistochemistry of Cx43 expression in tumors after WEC. Following WEC on the surface of tumor, cross sections of tumors were subjected to immunohistochemistry using an anti-Cx43 antibody and an Alexa Fluor 647 conjugated secondary antibody following observation with CLSM: (A) untreated tumor; (B) tumor subjected to WEC. Red indicates the intratumor expression of Cx43. Scale bars indicate 100 μm. (C) Fluorescence intensity of tumor cross sections was quantified by ImageJ software. Data are expressed as mean ± S.D (n > 3). *p < 0.05.

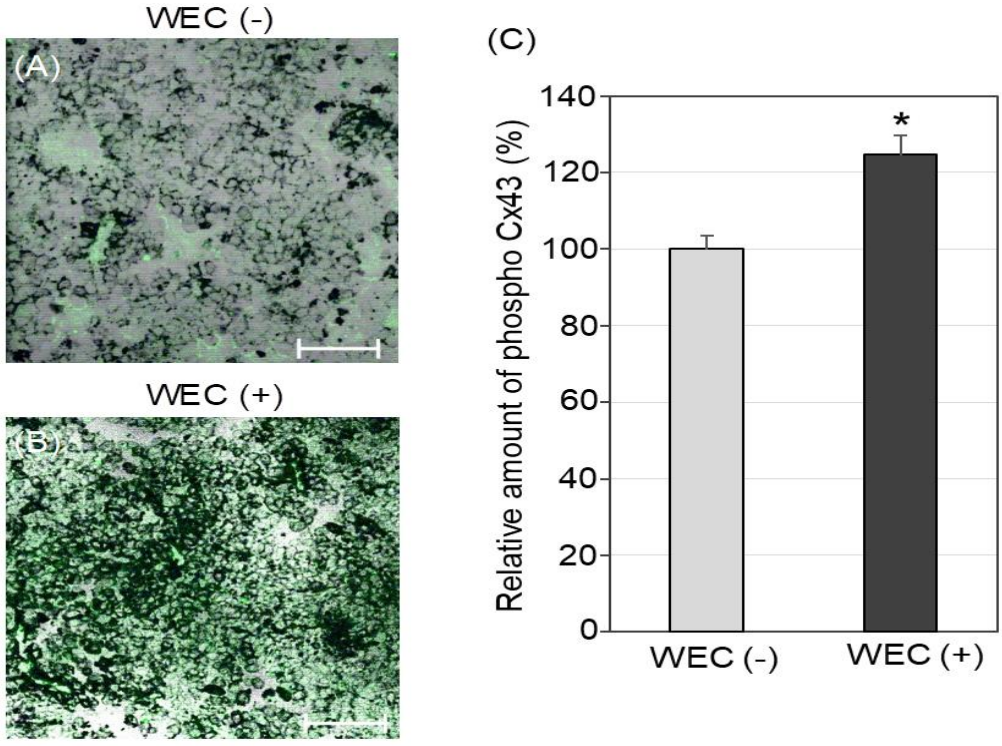

Fig. 4 Immunohistochemistry of Cx43 phosphorylation status in tumors after WEC. Following application of WEC on the surface of tumor, cross sections of various regions of tumors were subjected to immunohistochemistry using an anti-Cx43 (phospho Ser367) antibody and an Alexa Fluor 488 conjugated secondary antibody followed by observation with CLSM: (A) untreated tumor; (B) tumor subjected to WEC. Green indicates the phospho-Ser367 Cx43. Scale bars indicate 100 μm. (C) Fluorescence intensity of tumor cross sections was quantified by ImageJ software. Data are expressed as mean ± S.D (n > 3). *p < 0.05.

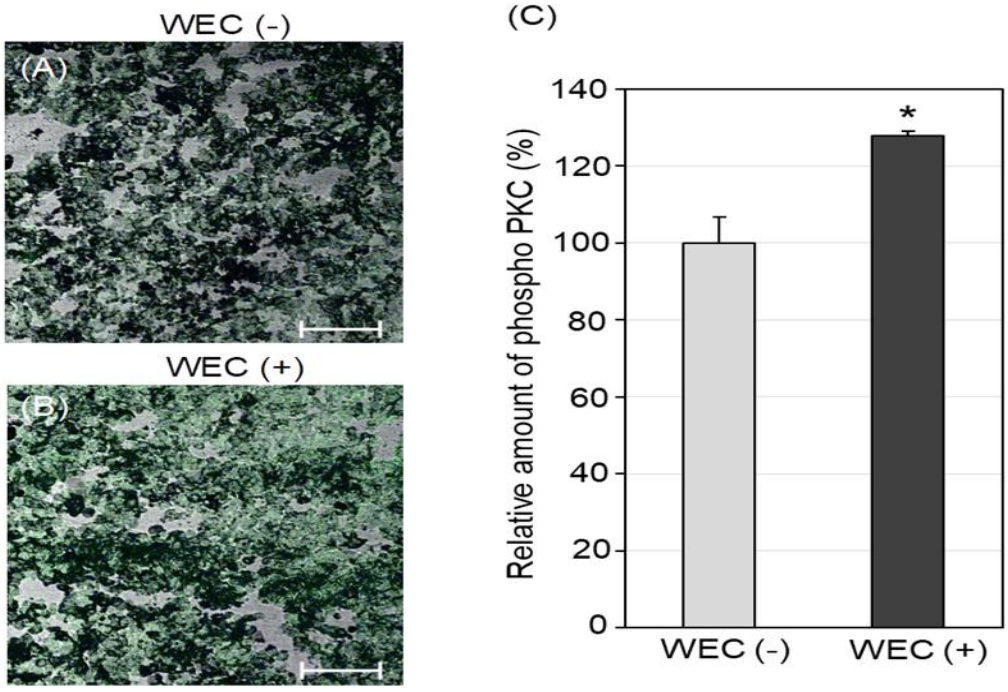

Fig. 5 Immunohistochemistry of activation of PKC in tumors by WEC. Following application of WEC on the tumor surface, cross sections of tumors were subjected to immunohistochemistry using an anti-PKC (phospho T497) antibody and an Alexa Fluor 488 conjugated secondary antibody, followed by observation with CLSM: (A) untreated tumor; (B) tumor subjected to WEC. Green indicates the phospho T497 PKC. Scale bars indicate 100 μm. (C) Fluorescence intensity of tumor cross sections was quantified by ImageJ software. Data are expressed as mean ± S.D ($n > 3$). *$p < 0.05$.

1.3.4 The effect of combination of DOX-NP and WEC on tumor growth in a mouse melanoma model

I investigated the effect of combination of DOX-NP and WEC on tumor growth in a mouse melanoma model. DOX-NP alone showed the significant suppression of the tumor growth by 65% and 71% compared to untreated control (WEC (-)) on day 14 and 17, respectively (Fig. 6). Furthermore, combination of DOX-NP with WEC (+) significantly inhibited the tumor growth by 80, 83 and 88 % on day 14, 17 and 20, respectively. The tumor volumes of the group treated with the combination of DOX-NP and WEC (+) were around 43 % compared to those of DOX-NP alone on day 14, 17

and 20. In addition, WEC treatment alone (WEC (+)) also reduced the tumor growth, although the effect of WEC (+) was not statistical significant (Fig. 6). This result suggests that weak electricity has the possibility of anticancer activity.

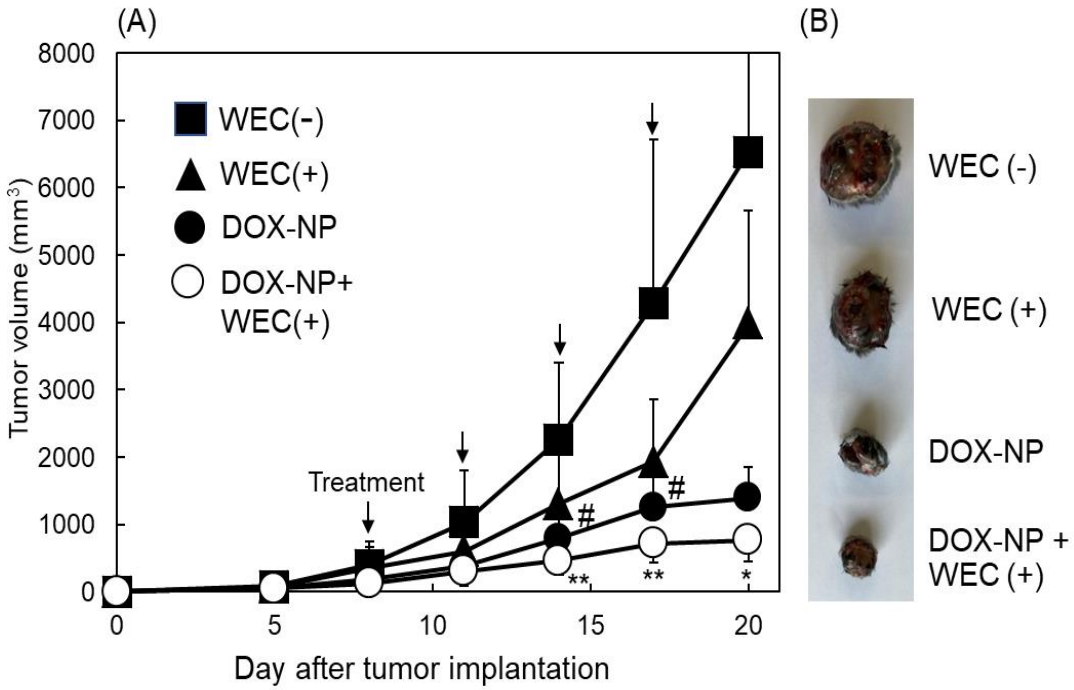

Fig. 6 Antitumor effect of DOX-NP combined with WEC in B16-F1 tumor-bearing mice. B16-F1 cells were injected subcutaneously in C57BL/6J mice at day 0. After cells inoculation, mice (n=24) were randomly divided into four groups and treated with WEC/DOX-NP/DOX-NP with WEC at the indicated time point (↓). The WEC (-) group did not receive any treatment. (A) Tumor growth is indicated as tumor volume measured twice in a week. Each value represents as mean ± SD for six mice from each group. *P<0.05, ** P<0.01 vs WEC (-) for (DOX-NP + WEC (+)); $^{\#}$ P<0.05 vs WEC (-) for (DOX-NP). (B) Representative image of dissected tumors at day 20.

1.3.5 The effect of WEC on cell proliferation and viability of B16-F1 melanoma cells

I investigated the effect of WEC on cell proliferation and viability of B16-F1 melanoma cells in vitro. I found that WEC without anticancer drug

prevented tumor growth. WEC (+) showed significant suppression of cell proliferation by 48% compared to untreated control (WEC (-))(Fig. 7 A), while there was no significant change in cell viability (%) between the two groups (Fig. 7 B). Thus, I expected that physical treatment (WEC) can be a new cancer treatment.

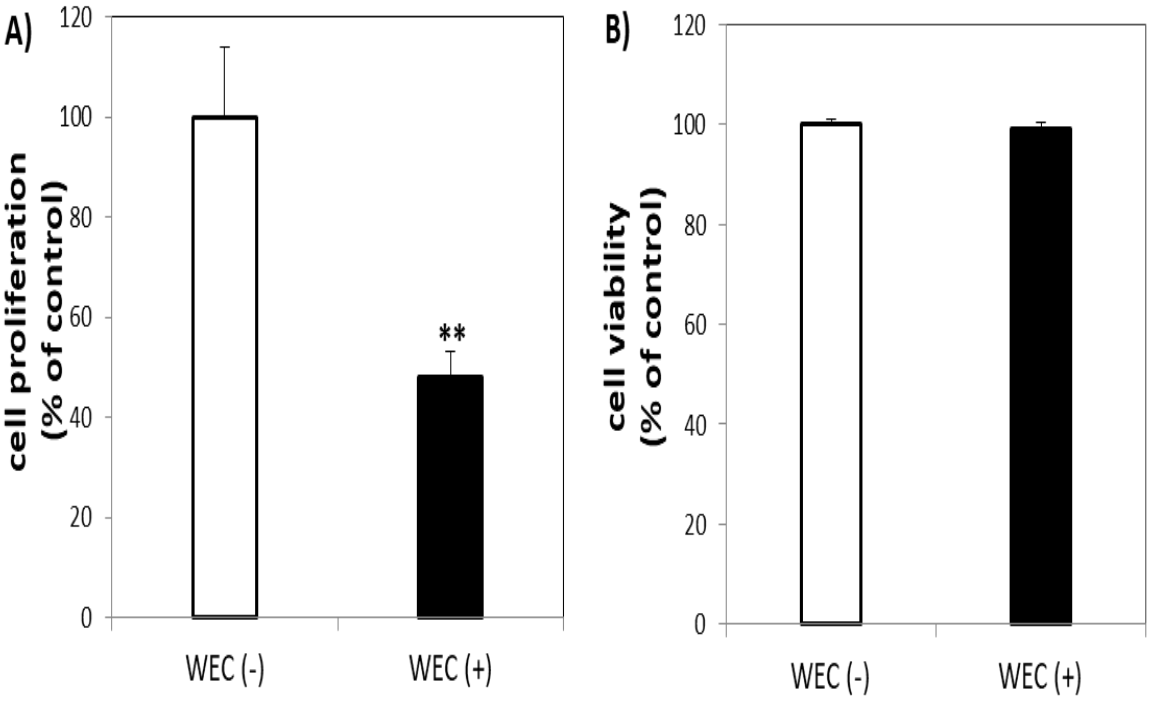

Fig. 7 The effect of WEC on cell proliferation and viability of B16-F1 melanoma cells. B16-F1 cells were cultivated at 1×10^5 cells per dish. Cells were treated with a constant current of 0.34 mA cm^{-2} for 15 min at 24 h and 48 h after cultivation and 24 h after last WEC, cells were collected and cell proliferation (A) and viability (B) was measured using trypan blue exclusion method. Data are expressed as the mean ± SD (n = 3). $**P < 0.01$ vs. untreated control (WEC (-)) group.

1.3.6 The effect of WEC on the expression levels of cyclin B1 protein in B16-F1 melanoma cells

Then, to clarify the mechanism behind the inhibitory effect of WEC on tumor cell growth, I focused on cycle B1 protein, an important regulator of cell division. It attaches to cyclin-dependent kinase (cdk1) to create a cyclin B/cdk1 complex. Once this complex is activated, it phosphorylates a crucial

set of proteins to initiate the events of mitosis **[158]**. I found that WEC treatment reduced the amount of cyclin B1 protein compared to not treated group, although the difference was non statistically significant.

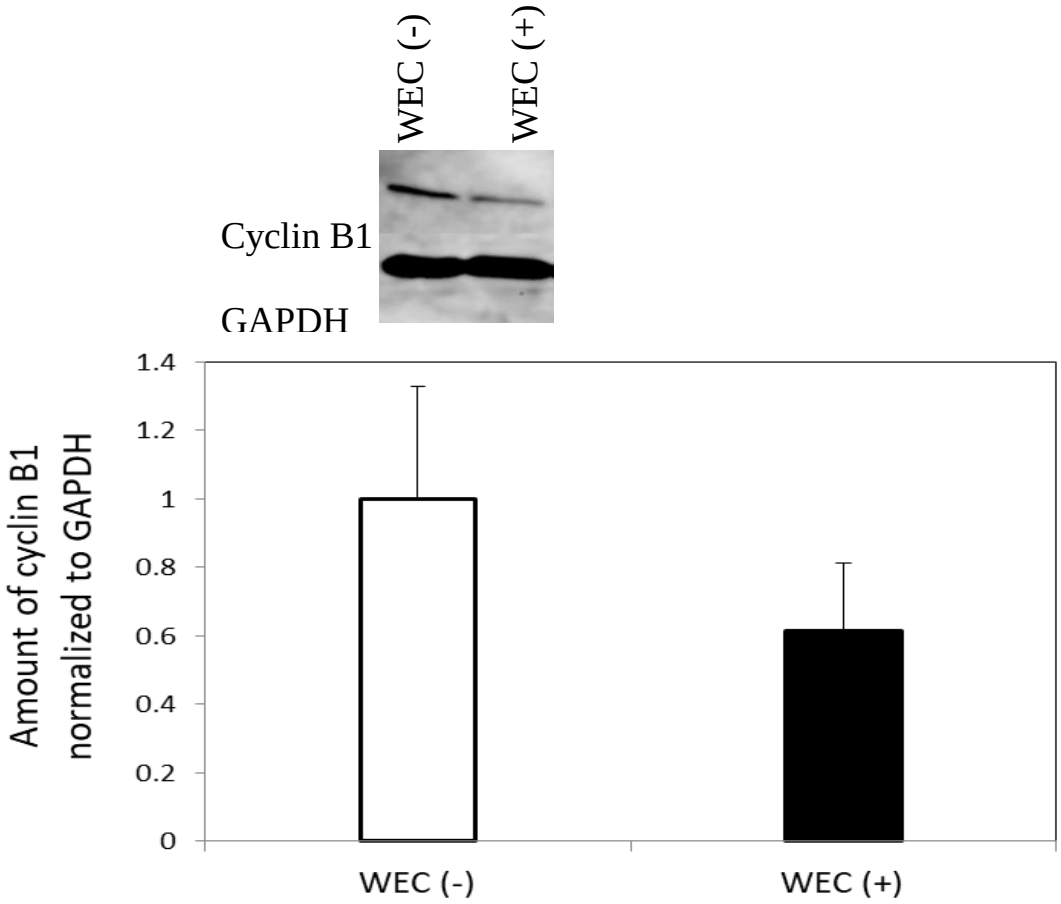

Fig. 8 The effect of WEC on the expression levels of cyclin B1 protein in B16-F1 melanoma cells. B16-F1 cells were cultivated at 1×10^5 cells per dish. Cells were treated with a constant current of 0.34 mA cm^{-2} for 15 min at 24 h and 48 h after cultivation and 24 h after last WEC, cells were collected for protein extraction and the expression levels of cyclin B1 protein was determined using western blotting analysis. Data are expressed as the mean ± SD (n > 3). P = 0.09 vs. untreated control (WEC (-)) group.

1.4 Discussion

I first examined the effect of WEC on the intratumor accumulation of DOX-NP. After IV administration of DiIC18-labeled DOX-NP into a tumor-bearing mouse, WEC was applied to the surface of the tumor. Quantitatively, the fluorescent intensity was significantly higher in WEC-treated tumors compared to untreated control tumors (Fig. 1). These results indicate that the intratumor accumulation of nanoparticles was dramatically increased following WEC, consistent with an augmentation of the EPR effect by WEC. Additionally, I examined the effect of WEC on the pharmacokinetics (blood retention of DOX-NP) after administration of DOX-NP to normal mouse without cancer inoculation. DOX concentrations in blood after intravenous injection of DOX-NP with or without WEC treatment were almost the same (Fig. 2). Therefore, I concluded that WEC hardly affected the pharmacokinetics (blood retention of DOX-NP) after administration of DOX-NP.

Next, I attempted to delineate the signaling events leading to improved intratumor accumulation of nanoparticles mediated by WEC. It has been reported that WEC stimulation on the skin surface causes a transport shunt for topically applied nanoparticles or drugs into the epidermis or dermis via a paracellular pathway **[152]**. This paracellular route was facilitated by WEC-mediated opening of intercellular junctions **[32,152]**. Among several candidate intercellular junctions, the proteins that form gap junctions are reported to be responsive to electric stimuli. For example, in the heart, gap junctions mediate rapid current transmission between adjacent cells, and they transmit presynaptic electrical currents to the postsynaptic sites in electrical synapses of neurons **[159,160]**. Furthermore, increased degradation of gap junctions in diabetic retinopathy is reported to contribute to endothelial cell dysfunction and causes leakage of the blood-retinal barrier **[161,162]**.

Therefore, to elucidate the mechanism of improved intratumor delivery and distribution of nanoparticles, I evaluated the expression levels and phosphorylation of the gap junction protein Cx43 in tumors following WEC. Interestingly, I found that WEC treatment significantly reduced the amount

of Cx43 by approximately 57% of control levels (Fig. 3) while it increased the amount of phosphorylated Cx43 by approximately 25% of control levels (Fig. 4). As Cx43 phosphorylation is reported to attenuate gap junction assembly and to potentially induce Cx43 degradation **[163]**, therefore, these results are consistent with an augmentation of the EPR effect via WEC-mediated opening of gap junctions within the tumor microenvironment. To further investigate gap junction formation following WEC, I examined the expression and phosphorylation of PKC, which colocalizes with and directly phosphorylates Cx43 **[164]**. Here, I found that phosphorylation of PKC was upregulated in the tumor immediately after application of WEC (Fig. 5). Quantitatively, the amount of phosphorylated PKC was increased by approximately 28% of control levels in WEC-treated tumors. Taken together, these results suggest that application of WEC on the tumor surface leads to activation of the signaling molecule PKC, followed by the phosphorylation of Cx43. Phosphorylated Cx43 promotes the dissociation of gap junctions and augmentation of the EPR effect. Regarding the WEC-induced change of the amount of Cx43 in the skin, it was suggested that regeneration of Cx43 protein might be occurred after decrease in the amount of Cx43 protein by enhancement of phosphorylation for recovering gap junction at 6 h after iontophoresis in our previous report **[32]**. Probably, regeneration of Cx43 protein in tumor occurs approximately 6 h after WEC treatment. Since the phosphorylation of PKC in tumor is a trigger event for change in intercellular junctions, this phenomenon would stop before Cx43 protein regeneration begins.

As WEC increased DOX-NP accumulation in the tumors (Fig. 1), I investigated the effect of combination of DOX-NP and WEC on tumor growth in a mouse melanoma model. DOX-NP alone showed the significant suppression of the tumor growth by 65% and 71% compared to untreated control (WEC (-)) on day 14 and 17, respectively (Fig. 6). Furthermore, combination of DOX-NP with WEC (+) significantly inhibited the tumor growth by 80, 83 and 88 % on day 14, 17 and 20, respectively. The tumor volumes of the group treated with the combination of DOX-NP and WEC (+) were around 43 % compared to those of DOX-NP alone on day 14, 17 and 20. Thus, although DOX-NP alone also inhibited tumor growth, the

combined application of DOX-NP with WEC (+) provided a more potent antitumor effect. This result is consistent with the improvement in intratumor accumulation of DOX-NP by WEC (Fig. 1). In addition, WEC treatment alone (WEC (+)) also reduced the tumor growth, although the effect of WEC (+) was not statistical significant (Fig. 6). This result suggests that weak electricity has the possibility of anticancer activity.

I found that WEC treatment alone (WEC (+)) reduced the tumor growth in melanoma bearing mice, although the effect of WEC (+) was not statistically significant (Fig. 6). Based on this finding, I evaluated the in vitro effect of WEC on cell proliferation and viability of B16-F1 melanoma cells. I found that cell proliferation was inhibited by WEC and cell viability was not affected. This result indicates that WEC has suppression effect of cancer cell proliferation without using anticancer agent. To elucidate the mechanism behind this result, I examined the effect of WEC on cyclin B1 protein expression. Cyclin B1, known as a mitotic cyclin, is a key component in the control of cell cycle progression from G2 to M phase and participates in cell growth, differentiation, and metastasis in various cancer types **[165-167]**. Fang et al. found that overexpression of Cyclin B1 promoted cell proliferation and tumor growth in human colorectal cancer **[168]**. My results revealed that WEC suppressed Cyclin B1 protein expression in B16-F1 melanoma cells, although this effect was not significant. So, this result suggests that the inhibitory effect of WEC on cell proliferation may be due to arresting the cell cycle by down-expression of cyclin B1.

Chapter II

Deleterious effect of thermal treatment on testicular tissue via alteration of sperm-specific calcium channels in rats

1.1 Introduction

Infertility is a health issue affecting approximately 15% of couples who have regular unprotected intercourse **[169]**. The latest WHO statistics indicate that approximately 50–80 million people suffer from infertility worldwide **[170,171]**. According to recent studies, 20–70% of infertility cases are attributed to male-related factors **[38,172]**.

The mammalian testis must be in the temperature range of 2–8 °C below the core body temperature for normal spermatogenesis and good testicular function **[173]**. A rise in testicular temperature may be harmful to spermatogenesis and, as a result, can cause infertility **[174,175]**. This condition is becoming more prevalent nowadays, as a result of occupational or lifestyle exposures such as prolonged driving or sitting, sauna use, and wearing tight-fitting underwear **[176,177]**. The testis exhibits a range of mechanisms in response to heat stress, including heat shock, oxidative stress, and apoptosis **[49,8]** and heat stress reduces sperm count and motility and causes an increase in an abnormal sperm percentage **[150]**. Additionally, heat stress induces apoptosis of the spermatogonial germ cells in the seminiferous tubules, resulting in lower sperm density, altered testicular morphology **[179,180]**, and consequently poor fertilization capacity both in vivo and in vitro.

Mammalian spermatozoa must proceed through a variety of challenges after ejaculation before fertilizing an egg **[181]**. These processes are usually stimulated by activation of ion channels expressed on the sperm membrane **[107,182]** , such as the cation channel of sperm (CatSper) channel complex, which consists of four pore-forming subunits (CatSper1–4) and five accessory subunits (β, δ, ε, γ, and ζ) **[183]**. CatSper1 and -2 are considered vital for flagellar beat and hyperactivated motility of sperm, whereas CatSper3 and -4 are involved in the acrosome reaction and egg coat penetration **[116,127,184]**. Any disruption in the functions of CatSper channels and associated genes will affect fertility in both humans and animals **[109,185]**.

Previous studies demonstrated downregulated expression of CatSper genes are in mice orally administrated bisphenol A **[186]**, cadmium **[187]**, dutasteride or nifedipine **[188]**. CatSper expression was also suppressed after oral methamphetamine administration in rats **[189]**, spinal cord injury in a mouse model **[133]**, and experimental varicocele in rats **[190]**. However, there have been no studies on the relationship between heat stress and CatSper gene expression. Thus, in this study, I investigated the changes in the gene expression of CatSper1, CatSper2, 3β-HSD as steroidogenesis marker, and BAX as apoptotic marker and in sperm parameters (motility, number, and abnormal sperm percentage) and testicular weight in heat-stressed rats at different time points. Additionally, I investigated the influence of single or repeated exposure to scrotal heating on the expression of CatSper1 and -2 genes in testicular tissue.

1.2 Materials and methods

1.2.1 Materials and animals

Chloral hydrate, 1% eosin Y solution and 10% neutral buffered formalin were purchased from FUJIFILM Wako Pure Chemical Corporation (Osaka, Japan). All other reagents used were of the highest grade commercially available. Eight-week-old male Wistar rats (180–200 g) were purchased from Japan SLC, Inc. (Shizuoka, Japan). All animal experiments were evaluated and approved by the Animal and Ethics Review Committee of Tokushima University.

1.2.2 Heat treatment of rat testes

The rats were randomly divided into two separate groups (control and heat-treated groups). In the heat-treated group, rats were anesthetized by intraperitoneal administration of chloral hydrate (400 mg/kg), and then the testes of rats were immersed in a thermostatically controlled water bath at 43°C for 30 min once daily for 6 days. Control group rats were treated in the same way, except the testes were immersed in a water bath maintained at 22°C. Then, the rats were killed by cervical dislocation at 1, 14, or 35 days after treatment according to Kanter et al. **[8]**, and the cauda epididymis and testis were collected to determine sperm parameters, testicular weight, and the expression of CatSper1, CatSper2, 3β-HSD, and BAX.

1.2.3 Characteristics of spermatozoa

The cauda epididymis was removed and placed in a sterilized petri dish containing 2 mL normal saline prewarmed to 37°C and was subsequently macerated to release epididymal contents in a suspension that was handled precisely like the semen **[191]**.

1.2.3.1 Sperm motility analysis

Sperm motility was analyzed according to the procedure by Slott et al., **[192]**. A drop of the epididymal suspension was placed on a prewarmed glass slide and covered with a prewarmed glass cover slide, which was then inspected under a light microscope (Axio Vert.A1, Carl Zeiss, Germany) to assess individual sperm motility. Several microscopic fields were examined to evaluate the percentage of motile spermatozoa.

1.2.3.2 Measurement of sperm count

The sperm cell concentration per milliliter of semen was determined as described by **[193]**. Semen was further diluted with normal saline, and a few drops of formalin were added to kill the spermatozoa. The sperm were counted using an improved Neubauer hemocytometer counting chamber (Matsunami Glass Ind, Ltd, Osaka, Japan).

1.2.3.3 Evaluation of abnormal sperm

The number of abnormal sperm was performed using the method of **[194]**. Briefly, one drop of semen was mixed with one drop of eosin stain. A smear was prepared, air-dried, examined under a light microscope. Abnormal sperm was recorded as a percentage (%) of the number of abnormal spermatozoa relative to the total sperm concentration.

1.2.4 mRNA Quantification using real-time RT-PCR

Total RNA was extracted from the testis and purified using NucleoSpin® RNA (Macherey-Nagel, Germany) according to the manufacturer's instructions. The total RNA concentration was measured using the Nanodrop 8000 (Thermo Fisher Scientific, Rockland, USA). cDNA was synthesized from 200 ng total RNA with PrimeScript RT Master Mix (Perfect Real Time, Takara Bio, Otsu, Japan) on the MJ Mini Personal Thermal Cycler (Bio-Rad, Hercules, CA, USA). The reverse transcription reaction was performed at 37°C for 15 min followed by 85°C for 5 s. Real-time RT-PCR

was performed using TB Green^{TM} Premix Ex TaqTM II (Tli RNaseH Plus, Takara Bio) and the Thermal Cycler Dice Real-Time System III (Takara Bio). To analyze the mRNA expression levels of CatSper 1, CatSper 2, 3β-HSD, BAX, and β-actin, the cDNA was denatured at 95°C for 30 s, followed by 40 cycles of 95°C for 5 s and 60°C for 30 s for amplification. The following primer sequences were used: CatSper1, (forward) 5′-TCTTGGAGCGATGAGGAC-3′) and (reverse) 5′-GACGATTGTGTCAGGCA-3′; CatSper2, (forward) 5′-TGGTTGTTGCTTGGT-3′ and (reverse) 5′-TTCCTTGACTGGTTCCTCT-3′; 3β-HSD, (forward) 5′ TCCCCAGTGTATGTAGGCAATGTGGC-3′ and (reverse) 5′-CCATTCCTTGCTCAGGGTGC-3′; BAX (forward) 5′-CGCGTGGTTGCCCTCTTCTACTTT-3′ and (reverse) 5′-CAAGCAGCCGCTCAACGGAGGA-3′; and β-actin, (forward) 5′-ACTATCGGCAATGAGCGGTTCC-3′ and (reverse) 5′-CTGTGTTGGCATAGAGGTCTTTACG-3′. CatSper1, CatSper2, 3β-HSD, and BAX mRNA levels were calculated using the $2^{-\Delta\Delta Ct}$ method and were normalized to those of β-actin.

1.2.5 Determination the effect of single or repeated heat exposure on the expression of CatSper 1 and-2 in rat testis

Based on the above condition, in which rat testes were subjected to six heat treatments at 43°C for 30 minutes (one per day for six days) at 43°C for 30 minutes, I further divided rats into three groups: the first, in which rat testes were subjected to a single heat treatment at 43°C for 30 minutes; the second, in which rat testes were subjected to two heat treatments at 43°C for 30 minutes (one per day for two days); and the third, in which rat testes were subjected to three heat treatments at 43°C for 30 minutes (one per day for three days). After that, the expression of CatSper 1 and-2 genes was measured at 1, and 14 days after treatment. In order to fix the incubation time after heat treatment in all experiment groups, rat testes were subjected to one, two, or three heat treatments at 43°C for 30 minutes, and the expression of CatSper 1 and-2 genes was measured at 7,

6, and 5 days after treatment and compared to the 1 day incubation time after six heat treatments.

1.2.6 Statistical analysis

One-way ANOVA followed by Tukey's post-hoc test was conducted for the statistical analysis. Data presented as the mean ± SD. P values < 0.05 are considered to indicate significance.

1.3 Results

1.3.1 The effect of heat treatment on testis weight at various time intervals

I first examined the effect of heat treatment on testis weight at various time intervals (Fig. 9). Treated rats exhibited a significant decrease in testis weight at 1 day after heat stress compared with control rats, and this decrease did not improve even after 14 and 35 days.

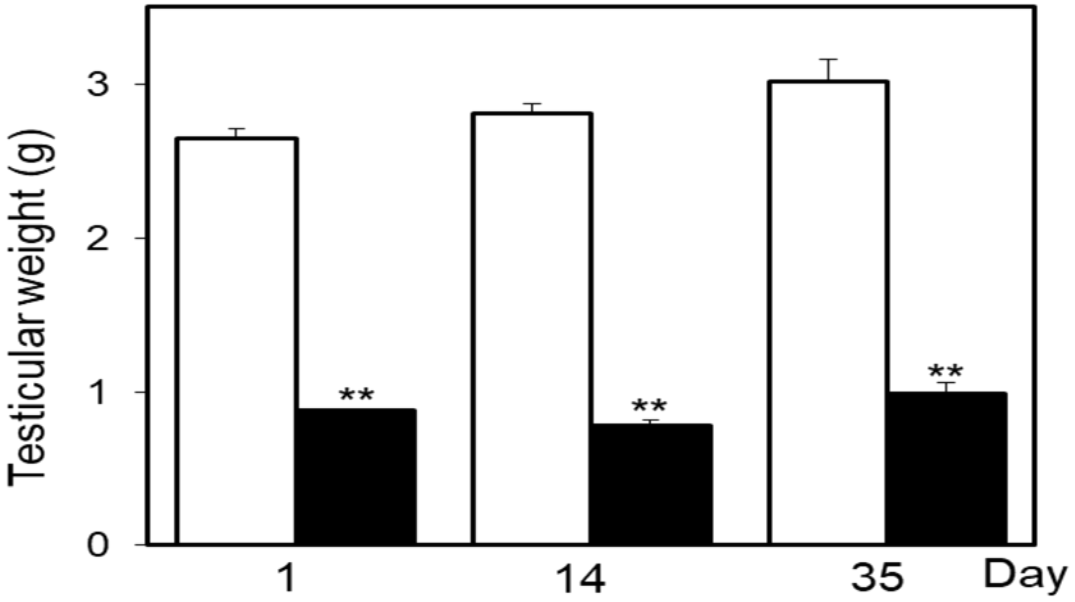

Fig. 9 Effect of heat treatment on testicular weight

The white and black columns indicate the testicular weight of the control and heat-treated rats, respectively. Data are presented as the mean ± SD of four rats from each group. ∗∗P < 0.01 vs. control group.

1.3.2 The effect of heat treatment on sperm parameters at different time points

Next, I investigated the effect of heat treatment on sperm parameters at different time points (Fig. 2). Heat treatment significantly decreased sperm motility at 1 and 14 days compared with the control group (Fig. 10A). Sperm count was also markedly decreased after heat treatment at 1 and 14 days

compared with the control group (Fig. 10B). Furthermore, there were a significant decrease in the percentage of normal sperm (Fig. 11A) and an obvious increase in the percentage of abnormal sperm (Fig. 11B–F) in the heat-stressed rats compared with the control rats at days 1 and 14 (Fig. 10C). We noted a cessation in sperm production at 35 days after heat treatment.

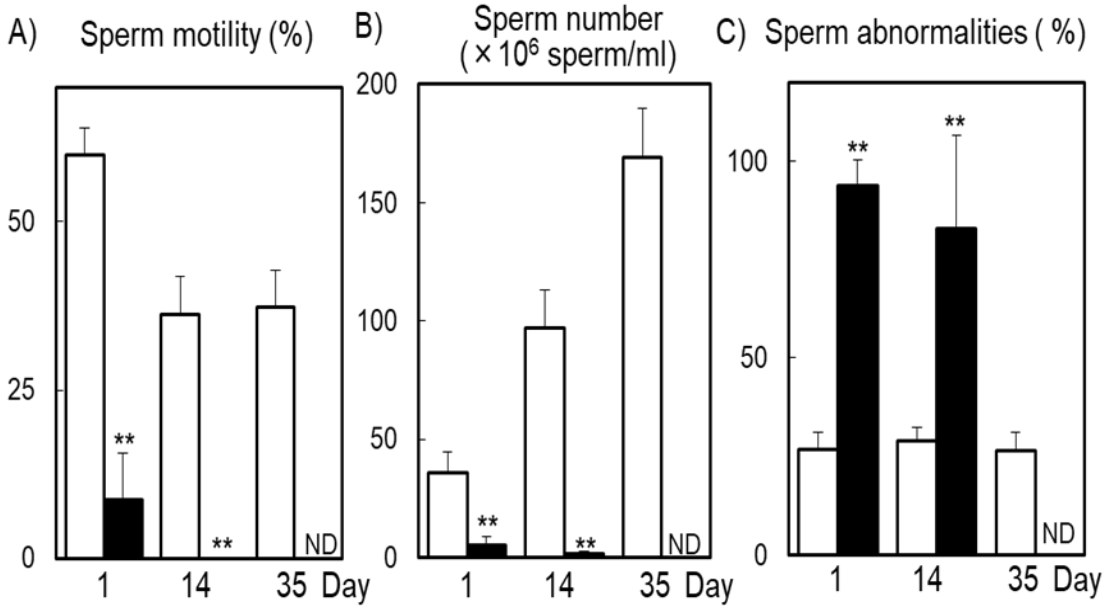

Fig. 10 Effect of heat treatment on sperm parameters

A) Sperm motility (%), (B) sperm number ($\times 10^6$ sperm/mL), and (C) abnormal sperm (%). The white and black columns indicate the sperm parameters of the control and heat-treated rats, respectively. Data are expressed as the mean ± SD of four rats from each group. $**P < 0.01$ vs. control group. (ND: no sperm detected).

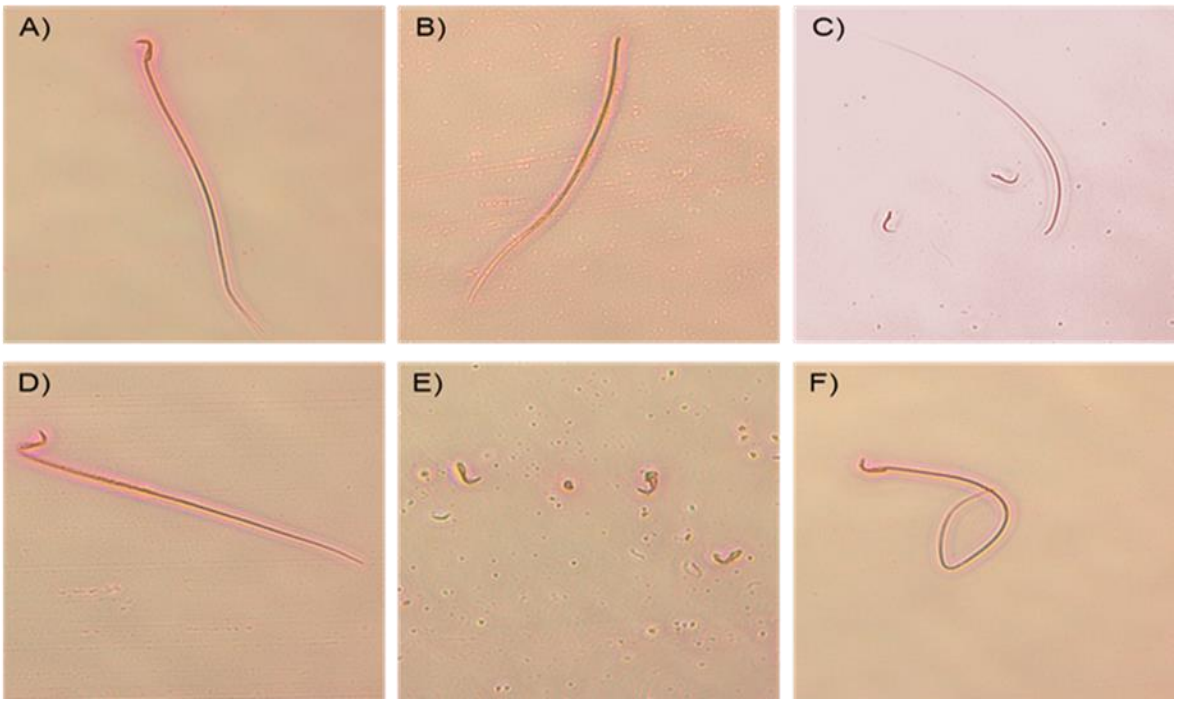

Fig. 11 Microphotographs of morphologically normal sperm and of various sperm abnormalities

(A) Normal rat sperm, (B) headless sperm, (C) detached head, (D) bent neck, (E) tailless sperm, and (F) coiled tail.

1.3.3 The effect of heat treatment on CatSper1 and -2, steroidogenesis and apoptosis genes expression at various time points

Then, I evaluated the influence of heat treatment on CatSper gene expression, steroidogenesis, and apoptosis gene expression in rat testes at various time points (Fig. 12). For the first time, I found a notable downregulation of CatSper1 expression in the heat-treated group compared with the control group on day 1, and this downregulation remained at 14 and 35 days after heat stress (Fig. 12A). I also observed a significant reduction in CatSper2 expression in heat-stressed rats compared with control rats, and the reduction was significantly greater on days 14 and 35 than on day 1 after heat stress, suggesting that CatSper2 downregulation occurred in a time-dependent manner (Fig. 12B). On the other hand, heat treatment resulted in significant upregulation of 3β-HSD expression at 14 and 35 days compared with the control group; its expression was also increased, but not significantly, on day 1 (Fig. 12C). BAX gene expression was increased in

rats exposed to heat stress compared with control rats, as soon as day 1, and this increase was maintained on days 14 and 35 (Fig. 12D).

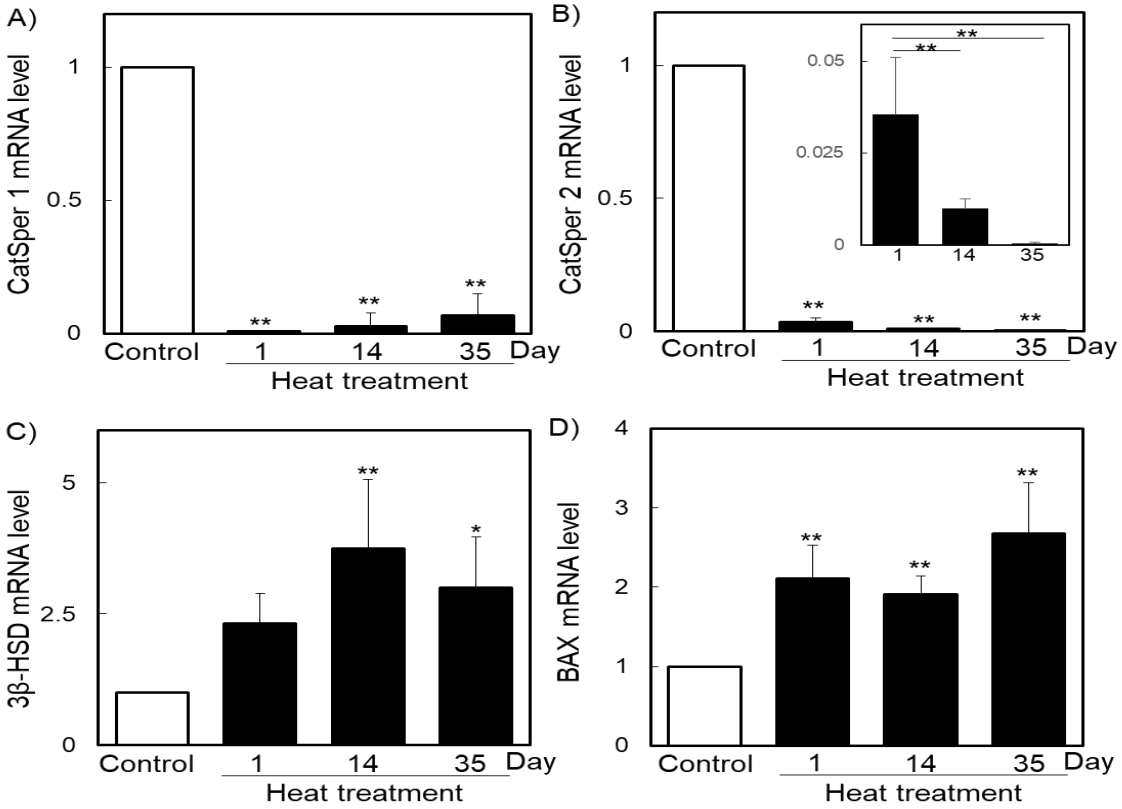

Fig. 12 The effect of heat treatment on the expression of certain genes in the rat testis

A) CatSper1, (B) CatSper2, (C) 3β-HSD, and (D) BAX. Data are presented as the mean ± SD of four rats from each group. ∗∗P < 0.01 vs. control group. ∗P < 0.05 vs. control group.

1.3.4 The effect of single or repeated heat exposure on the expression of CatSper 1 and-2 in rat testis

I found that rats exposed to scrotal heating at 43°C for 30 min for one and two times showed no significant change in CatSper1 and a significant reduction in CatSper2 gene expression on day 1 compared to the control group. Also, the expression of CatSper1 and-2 was downregulated in rats exposed to scrotal heating at 43°C for 30 min,

three, and six times, in comparison to the control group. Among the heat-treated groups, repeated exposure to heat treatment at 43°C for 30 min showed a gradual decrease in CatSper1 and-2 expression levels on day 1, while there was no significant change in CatSper1 between one and two-time treatment and no significant change in CatSper2 between two and three-time treatment on day 1 (Fig. 13A-B).

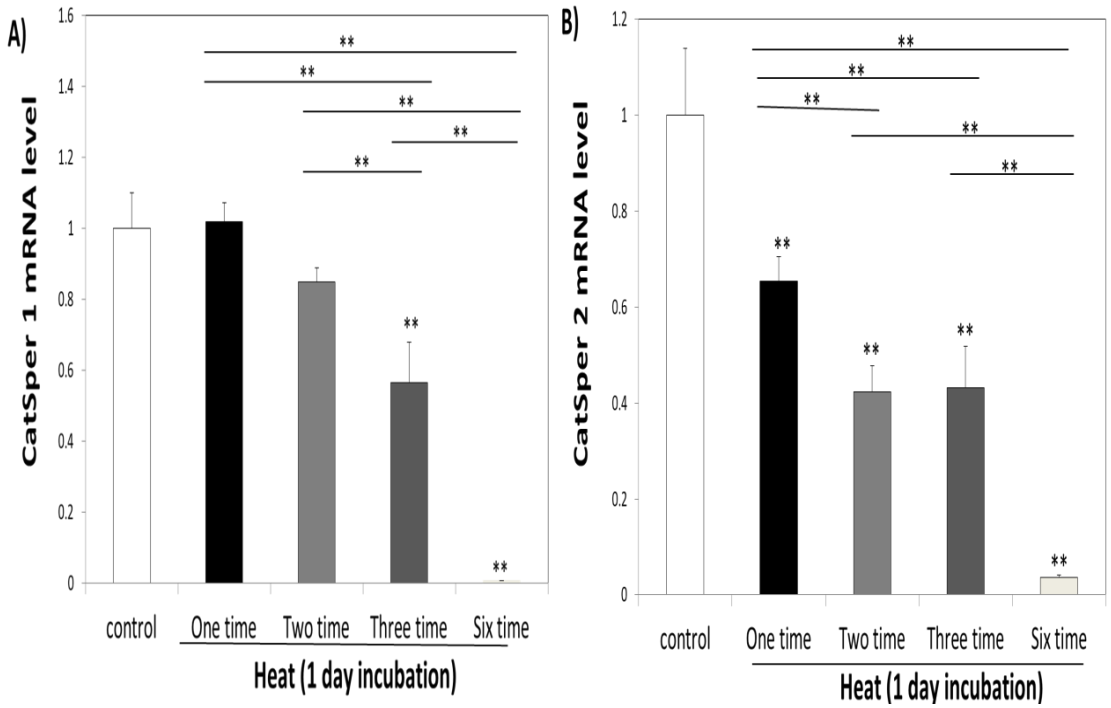

Fig. 13 The effect of single or repeated heat exposure on the expression of CatSper 1 and-2 in rat testis on day 1. Data are presented as the mean ± SD of three rats from each group. ∗∗P < 0.01 vs. control group.

On the other hand, rats subjected to heat treatment at 43°C for 30 min once, twice, three, or six times showed a significant reduction in CatSper1 and-2 mRNA levels on day 14 compared to the non-treated group. Among the heat-treated groups, two, three, and six-time treatments showed significant decreases in CatSper1 and-2 expression levels on day 14 compared to rats exposed to one-time heat. I noted that there was a non-significant change in CatSper1 gene expression on day 14 between two, three, and six-time exposure groups. Furthermore, rats exposed to three- and six-time heat had significantly lower levels of

CatSper2 expression on day 14 when compared to rats exposed to two-time heat (Fig. 14A-B).

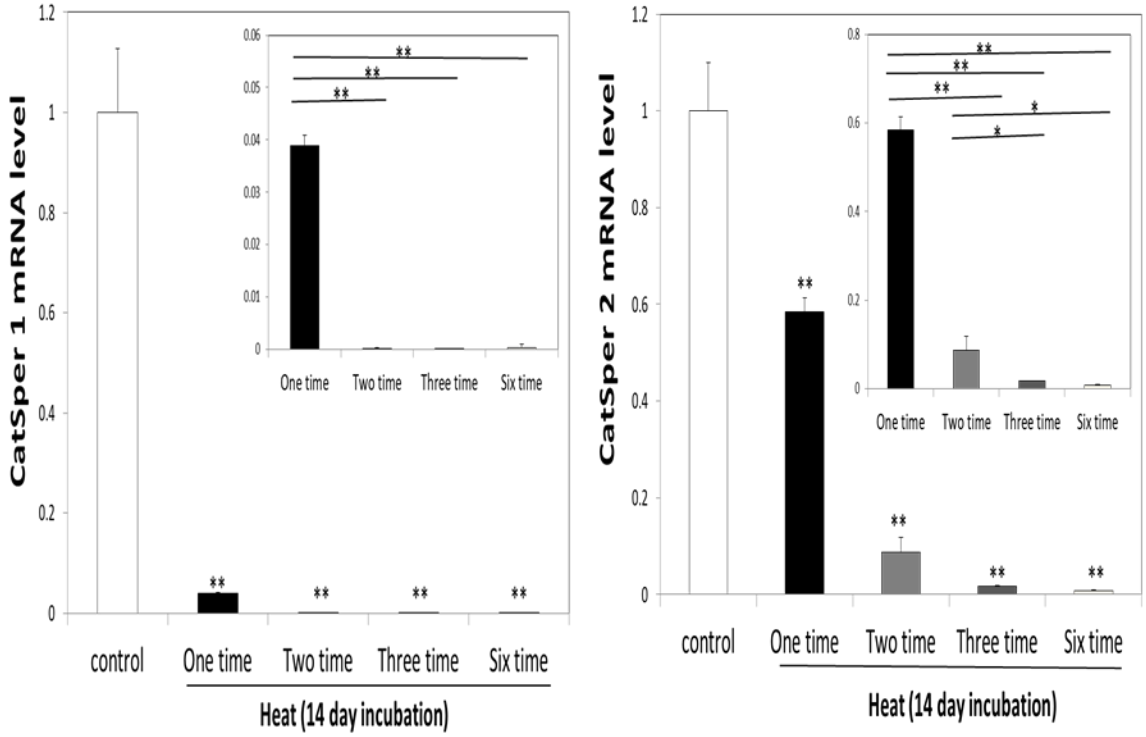

Fig. 14 The effect of single or repeated heat exposure on the expression of CatSper 1 and-2 in rat testis on day 14. Data are presented as the mean ± SD of three rats from each group. ∗∗P < 0.01 vs. control group. ∗P < 0.05 vs. control group.

I also found that after fixing the incubation time after heat treatment in the four experimental groups, rats subjected to heat treatment at 43°C for 30 min once, twice, three, or six times showed a significant reduction in CatSper1 and-2 mRNA levels compared to the control group. Among the heat-treated groups, two, three, and six-time treatments showed significant decreases in CatSper1 and-2 expression levels compared to rats exposed to one-time heat.

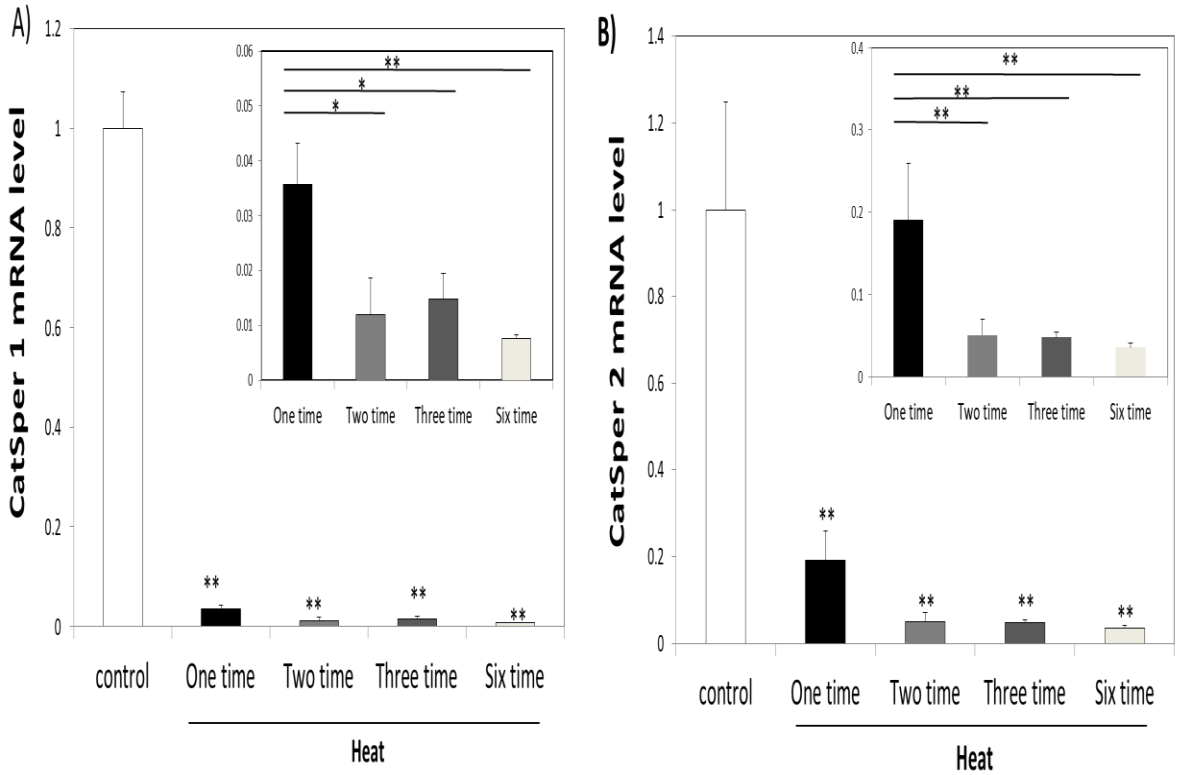

Fig. 15 The effect of single or repeated heat exposure on the expression of CatSper 1 and-2 in rat testis at fixed incubation time. The expression of CatSper 1 and-2 genes was measured at 7, 6, and 5 days after one, two, and three treatments, respectively, to resemble 1 day of incubation time after six heat treatments. Data are presented as the mean ± SD of three rats from each group. ∗∗P < 0.01 vs. control group. ∗P < 0.05 vs. control group.

1.4 Discussion

In this study, I first examined the effects of heat stress on testis weight and sperm characteristics (motility, number, and abnormalities). Testicular weight was significantly reduced in heat-stressed rats compared with control rats at 1, 14, and 35 days. This finding is consistent with that of Hand et al. **[195]** who observed testicular weight loss in adult male mice starting at 1 week after heat shock and persisting for at least 3 weeks. Sailer et al. **[196]** reported that the testicular weight of mice exposed to 42°C for 60 min decreased significantly, even until 35 days after exposure. According to Nicolino and Forest **[197]**, the reduction in testicular weight may be due to decreased numbers of Sertoli and germ cells within the seminiferous epithelium. Gasinska and Hilli **[198]** suggested that heat can cause denaturation of some cytoplasmic bridges in the syncytium, which can lead to degeneration of neighboring cells. Furthermore, Rasooli et al. **[179]** reported that heat stress increases apoptosis of spermatozoa, which leads to reduced testis and epididymis weights.

Sperm density and mobility are crucial factors for male fertility **[199]**. The present results showed decreases in sperm motility and number and an increase in the percentage of abnormal sperm in rats exposed to high temperatures after 1 and 14 days, with cessation of sperm production at 35 days. These findings accord with those Mahdivand et al. **[200]**, who observed significant decreases in sperm concentration, count, and viability and in fertility and an increase in chromatin abnormalities after heat stress. Rams subjected to scrotal insulation showed reduced sperm motility and an increased number of sperm with head or midpiece abnormalities, starting 2 weeks after the initiation of insulation and lasting 3 weeks **[201]**. The decrease in sperm quality could be due to damage of the sperm plasma membrane by overproduction of reactive oxygen species stimulated by heat stress. Spermatozoa are vulnerable to reactive oxygen species due to the high level of polyunsaturated fatty acids in their plasma membrane **[202]**.

Next, I investigated the effect of heat stress on the expression of CatSper1 and -2 genes in rat testis. In both mice and humans, the CatSper gene family is expressed mainly in the testis and plays a key role in sperm motility and male fertility **[109,203]**. Reduced CatSper channel expression in sperm may impede sperm motility and hyperactivity, leading to male infertility **[129**]. The CatSper genes are crucial for mammalian fertilization, and based on my results, CatSper1 and -2 expression levels were downregulated in testicular tissue at 1, 14, and 35 days after heat stress. Based on these findings, I additionally investigated the effect of the effect of single or repeated heat exposure on the expression of CatSper 1 and-2 in rat testis. I found that alteration of CatSper 1 and-2 mRNA levels showed a gradual decrease between the heat treated groups on day 1. On day 14, there was a significant reduction in CatSper 1 and-2 gene expression in the heat treated groups compared to the control group. Also, there was no significant change in CatSper 1 and-2 gene expression between two, three, and six-time treatments. However, two, three, and six-time treatments showed a significant decrease compared to one-time treatments at day 14 and fixed incubation times. These findings indicated that the suppression of the expression of CatSper 1 and-2 in rat testis after heat treatment was dependent on time despite the frequency of heat exposure as they decreased with increasing incubation time except for one-time treatment. Furthermore, my findings are consistent with a prior study in which the use of oral methamphetamine reduced the expression of these genes in a rat model **[204]**. Rezaian et al. **[133]** also revealed that the gene expression of CatSper1 and -2, but not CatSper3 and -4, was decreased at 2 weeks after spinal cord injury in a mouse model. The authors hypothesized that one of the causes of reduced sperm motility in this spinal cord injury mouse model was the downregulated CatSper1 and -2 expressions. Infertile men with asthenozoospermia exhibit similar reductions in CatSper1–4 gene expression as well as CatSper1 and -2 protein expression **[205]**. Conversely, CatSper1 or -2 null mouse spermatozoa showed impaired sperm motility, aberrant flagellar beating, and lack of hyperactivity and acrosome reaction, culminating in overall infertility **[109,113,206]**.

I also examined the effect of heat stress on 3β-HSD and BAX expression in rat testis as marker of steroidogenesis and apoptosis, respectively. Synthesis of testosterone in the testis is essential for normal spermatogenesis **[99]**. The expression of highly regulated genes, such as 17β-HSD3 and 3β-HSD, was shown to be critical for precise testosterone synthesis **[174]**. My findings revealed a significant increase in the expression of 3β-HSD at days 14 and 35 and a non-significant increase at day 1 in heat-stressed rats compared with control rats. These results are consistent with those of Shiraishi et al. **[207]**, who found that elevated scrotal temperature upregulates testosterone in patients, possibly to reduce testicular oxidative stress-mediated apoptosis. Furthermore, testosterone levels were highest on day 4 after heat stress, which indicates that mice may stimulate the hypothalamic-pituitary-Leydig cell axis to protect germ cells from heat damage **[208]**.

I observed significant upregulation of BAX expression at 1, 14, and 35 days after heat exposure. My results were similar to those of Delkhosh et al. **[89]**, who reported increased mRNA expression of caspase 3 and Bax in the testicular tissue of rats immersed in a water bath at 43°C for 20 min every other day for 8 weeks. This was due to heat stress, which can cause protein and DNA damage in the testicles and enhance the rates of cellular injury and apoptosis **[8]**.

Conclusion

Conclusion

From the results of this thesis, I concluded that the application of two different physical treatments (WEC and thermal treatment) inhibited cell growth in tumor and testicular tissue, but the mechanism is different. WEC enhanced the EPR effect of an anticancer drug through opening intracellular junctions in tumors and has a direct suppression effect on cancer cell proliferation. On the other hand, thermal treatment reduced testicular weight and induced significant deterioration of sperm motility, which was correlated with reduced CatSper gene expression and this finding shed light on one of the mechanisms underlying male infertility caused by heat stress and suggest new concepts for further therapeutic strategies.

Acknowledgement

Acknowledgement

First and foremost, to the almighty god, ALLAH, who has granted me all the graces to fulfill this work, supported me and blessed me by his mercy in all my life. I extended my heartfelt thanks to him. I would like to thank a number of people for their help and support during the production of this thesis.

I would like to express my sincere gratitude to my supervisor, Prof. Dr. Kentaro Kogure, Department of Pharmaceutical Health Chemistry, Graduate School of Pharmaceutical Sciences, the University of Tokushima, for his noble guidance, valuable suggestions, patience, support with full encouragement and enthusiasm throughout my study period.

I am extremely thankful to Dr. Mizune Ozono, Department of Pharmaceutical Health Chemistry, Graduate School of Pharmaceutical Sciences, the University of Tokushima, and Dr. Tatsuya Fukuta, School of Pharmaceutical Sciences, Wakayama Medical University, for their kind help and support.

A very special thanks to my classmates and students in the Department of Pharmaceutical Health Chemistry, Graduate School of Pharmaceutical Sciences, at the University of Tokushima for their friendship, help, and support during this work.

I am extremely grateful to the ministry of higher education of the Arab Republic of Egypt for financial support during my PHD period.

My warmest thanks go to my lovely wife, Esraa, and my son, Malek, who always encourage me with passion and endless support. I am so lucky to have a woman love me so much and stand beside me. I want to thank my faithful brothers and sisters who have always helped me and believed that I could do it.

I would like to dedicate this thesis to my dear mother, who has given me endless love and encouragement throughout my life, not only during this period. I also want to dedicate it to my deceased father, whom I missed so much and wish he was by my side at this moment.

References

References

[1] E.L. Spierings, J.A. Brevard, N.P. Katz, Two-minute skin anesthesia through ultrasound pretreatment and iontophoretic delivery of a topical anesthetic: a feasibility study, Pain Medicine 9 (2008) 55-59.

[2] J.B. Sloan, K. Soltani, Iontophoresis in dermatology: a review, Journal of the American Academy of Dermatology 15 (1986) 671-684.

[3] S. Roussakow, The history of hyperthermia rise and decline, Conference Papers in Science, Hindawi, 2013.

[4] K. Wang, J.E. Tepper, Radiation therapy-associated toxicity: Etiology, management, and prevention, CA: a cancer journal for clinicians 71 (2021) 437-454.

[5] M. Claire, MRI Guided Focused Ultrasound Surgery (FUS) of uterine leiomyomas: A Feasability Study, Workshop of MRI Guided: Focused Ultrasound Surgery, Syllabus, International Societ of Magnetic Resonance in Medicine, 2002.

[6] J. Ninet, X. Roques, R. Seitelberger, C. Deville, J.L. Pomar, J. Robin, O. Jegaden, F. Wellens, E. Wolner, C. Vedrinne, Surgical ablation of atrial fibrillation with off-pump, epicardial, high-intensity focused ultrasound: results of a multicenter trial, The Journal of thoracic and cardiovascular surgery 130 (2005) 803. e801-803. e808.

[7] H.C. Klingler, M. Susani, R. Seip, J. Mauermann, N. Sanghvi, M.J. Marberger, A novel approach to energy ablative therapy of small renal tumours: laparoscopic high-intensity focused ultrasound, European urology 53 (2008) 810-818.

[8] M. Kanter, C. Aktas, M. Erboga, Heat stress decreases testicular germ cell proliferation and increases apoptosis in short term: an immunohistochemical and ultrastructural study, Toxicology and industrial health 29 (2013) 99-113.

[9] M. Kanter, Y. Topcu-Tarladacalisir, S. Parlar, Antiapoptotic effect of L-carnitine on testicular irradiation in rats, Journal of molecular histology 41 (2010) 121-128.

[10] N.K. Lohiya, Reproductive Functions and Toxicology Following Scrotal Ultrasound Therapy in Rats, Int. J. Sci. Res. in Biological Sciences Vol 7 (2020).

[11] B. Barry, Drug delivery routes in skin: a novel approach, Advanced drug delivery reviews 54 (2002) S31-S40.

[12] O.D. Uitto, H.S. White, Electroosmotic pore transport in human skin, Pharmaceutical research 20 (2003) 646-652.

[13] H. Inada, A.-H. Ghanem, W.I. Higuchi, Studies on the effects of applied voltage and duration on human epidermal membrane alteration/recovery and the resultant effects upon iontophoresis, Pharmaceutical research 11 (1994) 687-697.

[14] D. Marro, Y.N. Kalia, M. Begoña Delgado-Charro, R.H. Guy, Contributions of electromigration and electroosmosis to iontophoretic drug delivery, Pharmaceutical research 18 (2001) 1701-1708.

[15] K.A. Walters, J. Hadgraft, Pharmaceutical skin penetration enhancement, Informa Health Care1993.

[16] J.E. Riviere, M.C. Heit, Electrically-assisted transdermal drug delivery, Pharmaceutical research 14 (1997) 687-697.

[17] V. Dhote, P. Bhatnagar, P.K. Mishra, S.C. Mahajan, D.K. Mishra, Iontophoresis: a potential emergence of a transdermal drug delivery system, Scientia pharmaceutica 80 (2012) 1-28.

[18] H.E. Bodde, J.C. Verhoef, M. Ponec, Transdermal peptide delivery, Biochemical Society Transactions 17 (1989) 943-945.

[19] J. Phipps, R. Padmanabhan, G. Lattin, Iontophoretic delivery model inorganic and drug ions, Journal of pharmaceutical sciences 78 (1989) 365-369.

[20] Y.N. Kalia, A. Naik, J. Garrison, R.H. Guy, Iontophoretic drug delivery, Advanced drug delivery reviews 56 (2004) 619-658.

[21] N.H. Bellantone, S. Rim, M. Francoeur, B. Rasadi, Enhanced percutaneous absorption via iontophoresis I. Evaluation of an in vitro system and transport of model compounds, International journal of pharmaceutics 30 (1986) 63-72.

[22] L.L. Miller, G.A. Smith, Iontophoretic transport of acetate and carboxylate ions through hairless mouse skin. A cation exchange membrane model, International journal of pharmaceutics 49 (1989) 15-22.

[23] B. Berner, S.M. Dinh, Electronically controlled drug delivery, CRC Press2019.

[24] S.B. Tiwari, N. Udupa, Investigation into the potential of iontophoresis facilitated delivery of ketorolac, International journal of pharmaceutics 260 (2003) 93-103.

[25] K. Sung, J.-Y. Fang, O.Y.-P. Hu, Delivery of nalbuphine and its prodrugs across skin by passive diffusion and iontophoresis, Journal of Controlled Release 67 (2000) 1-8.

[26] O. Siddiqui, M.S. Roberts, A.E. Polack, The effect of iontophoresis and vehicle pH on the in-vitro permeation of lignocaine through human stratum corneum, Journal of pharmacy and pharmacology 37 (1985) 732-735.

[27] S. Thysman, V. Préat, M. Roland, Factors affecting iontophoretic mobility of metoprolol, Journal of pharmaceutical sciences 81 (1992) 670-675.

[28] R.R. Burnette, B. Ongpipattanakul, Characterization of the pore transport properties and tissue alteration of excised human skin during iontophoresis, Journal of pharmaceutical sciences 77 (1988) 132-137.

[29] W.J. Shriber, A.L. Watkins, A manual of electrotherapy, Lea & Febiger1975.

[30] Y.W. Chien, O. Siddiqui, W.-M. Shi, P. Lelawongs, J.-C. Liu, Direct current iontophoretic transdermal delivery of peptide and protein drugs, Journal of pharmaceutical sciences 78 (1989) 376-383.

[31] T. Bagniefski, R.R. Burnette, A comparison of pulsed and continuous current iontophoresis, Journal of controlled release 11 (1990) 113-122.

[32] S. Hama, Y. Kimura, A. Mikami, K. Shiota, M. Toyoda, A. Tamura, Y. Nagasaki, K. Kanamura, K. Kajimoto, K. Kogure, Electric stimulus opens intercellular spaces in skin, Journal of Biological Chemistry 289 (2014) 2450-2456.

[33] M. Hasan, N. Tarashima, K. Fujikawa, T. Ohgita, S. Hama, T. Tanaka, H. Saito, N. Minakawa, K. Kogure, The novel functional nucleic acid iRed effectively regulates target genes following cytoplasmic delivery by faint electric treatment, Science and Technology of advanced MaTerialS 17 (2016) 554-562.

[34] K. Kigasawa, K. Kajimoto, S. Hama, A. Saito, K. Kanamura, K. Kogure, Noninvasive delivery of siRNA into the epidermis by iontophoresis using an atopic dermatitis-like model rat, International journal of pharmaceutics 383 (2010) 157-160.

[35] K. Kigasawa, K. Kajimoto, T. Nakamura, S. Hama, K. Kanamura, H. Harashima, K. Kogure, Noninvasive and efficient transdermal delivery of CpG-oligodeoxynucleotide for cancer immunotherapy, Journal of controlled release 150 (2011) 256-265.

[36] T. Fukuta, Y. Oshima, K. Michiue, D. Tanaka, K. Kogure, Non-invasive delivery of biological macromolecular drugs into the skin by iontophoresis and its application to psoriasis treatment, Journal of Controlled Release 323 (2020) 323-332.

[37] T. Fukuta, D. Tanaka, S. Inoue, K. Michiue, K. Kogure, Overcoming thickened pathological skin in psoriasis via iontophoresis combined with tight junction-opening peptide AT1002 for intradermal delivery of NF-κB decoy oligodeoxynucleotide, International Journal of Pharmaceutics 602 (2021) 120601.

[38] A. Agarwal, A. Mulgund, A. Hamada, M.R. Chyatte, A unique view on male infertility around the globe, Reproductive biology and endocrinology 13 (2015) 1-9.

[39] J.L. Evers, Female subfertility, The lancet 360 (2002) 151-159.

[40] V. Chang, L. Heutte, C. Petitjean, S. Härtel, N. Hitschfeld, Automatic classification of human sperm head morphology, Computers in biology and medicine 84 (2017) 205-216.

[41] E. Seli, D. Sakkas, Spermatozoal nuclear determinants of reproductive outcome: implications for ART, Human reproduction update 11 (2005) 337-349.

[42] A. Jung, H.C. Schuppe, Influence of genital heat stress on semen quality in humans, Andrologia 39 (2007) 203-215.

[43] T. Janowski, R. Sic, V. Vergles, Effect of air cooling power on temperature of scrotum skin and certain characteristics of bulls' semen in summer, Acta Agr Silvestria Ser Zootech (1971).

[44] S.K. Maloney, D. Mitchell, Regulation of ram scrotal temperature during heat exposure, cold exposure, fever and exercise, The Journal of Physiology 496 (1996) 421-430.

[45] A. Shafik, The cremasteric muscle. Role in varicocelogenesis and in thermoregulatory function of the testicle, Investigative Urology 11 (1973) 92-97.

[46] R. Cook, G. Coulter, J. Kastelic, The testicular vascular cone, scrotal thermoregulation, and their relationship to sperm production and seminal quality in beef bulls, Theriogenology 41 (1994) 653-671.

[47] A. Holstein, G. Orlandini, H. Baumgarten, Morphological analysis of tissue components in the tunica dartos of man, Cell and Tissue Research 154 (1974) 329-344.

[48] N. Blazquez, S. Long, T. Mayhew, G. Perry, N. Prescott, C. Wathes, Rate of discharge and morphology of sweat glands in the perineal,

lumbodorsal and scrotal skin of cattle, Research in veterinary science 57 (1994) 277-284.

[49] C. Paul, S. Teng, P.T. Saunders, A single, mild, transient scrotal heat stress causes hypoxia and oxidative stress in mouse testes, which induces germ cell death, Biology of reproduction 80 (2009) 913-919.

[50] J. Rock, D. Robinson, Effect of induced intrascrotal hyperthermia on testicular function in man, American journal of obstetrics and gynecology 93 (1965) 793-801.

[51] R. Munkelwitz, B.R. GILBERT, Are boxer shorts really better? A critical analysis of the role of underwear type in male subfertility, The Journal of urology 160 (1998) 1329-1333.

[52] S. Shefi, P.E. Tarapore, T.J. Walsh, M. Croughan, P.J. Turek, Wet heat exposure: a potentially reversible cause of low semen quality in infertile men, International braz j urol 33 (2007) 50-57.

[53] Y. Sheynkin, M. Jung, P. Yoo, D. Schulsinger, E. Komaroff, Increase in scrotal temperature in laptop computer users, Human reproduction 20 (2005) 452-455.

[54] R. Ivell, Lifestyle impact and the biology of the human scrotum, Reproductive biology and endocrinology 5 (2007) 1-8.

[55] S. Kumar, S. Zaidi, A. Gautam, L. Dave, H. Saiyed, Semen quality and reproductive hormones among welders—A preliminary study, Environmental health and preventive medicine 8 (2003) 64-67.

[56] P. Thonneau, B. Ducot, L. Bujan, R. Mieusset, A. Spira, Effect of male occupational heat exposure on time to pregnancy, International journal of andrology 20 (1997) 274-278.

[57] L. Bujan, M. Daudin, J.-P. Charlet, P. Thonneau, R. Mieusset, Increase in scrotal temperature in car drivers, Human Reproduction 15 (2000) 1355-1357.

[58] L.D. Russell, R.A. Ettlin, A.P.S. Hikim, E.D. Clegg, Histological and histopathological evaluation of the testis, Wiley Online Library, 1993.

[59] M.H. Perrard, M. Vigier, A. Damestoy, C. Chapat, D. Silandre, B.B. Rudkin, P. Durand, β-nerve growth factor participates in an auto/paracrine pathway of regulation of the meiotic differentiation of rat spermatocytes, Journal of cellular physiology 210 (2007) 51-62.

[60] K. Shiraishi, Heat and oxidative stress in the germ line, Studies on men's health and fertility, Springer2012, pp. 149-178.

[61] Y.-H. Lue, A.P. Sinha Hikim, R.S. Swerdloff, P. Im, K.S. Taing, T. Bui, A. Leung, C. Wang, Single exposure to heat induces stage-specific germ cell apoptosis in rats: role of intratesticular testosterone on stage specificity, Endocrinology 140 (1999) 1709-1717.

[62] E. Carlsen, A.M. Andersson, J.H. Petersen, N.E. Skakkebæk, History of febrile illness and variation in semen quality, Human Reproduction 18 (2003) 2089-2092.

[63] R. Mieusset, L. Bujan, C. Mondinat, A. Mansat, F. Pontonnier, H. Grandjean, Association of scrotal hyperthermia with impaired spermatogenesis in infertile men, Fertility and sterility 48 (1987) 1006-1011.

[64] N.H.I. Hjollund, J.P.E. Bonde, T.K. Jensen, J. Olsen, D.F.P.P.S. Team, Diurnal scrotal skin temperature and semen quality, International journal of andrology 23 (2000) 309-318.

[65] G. Brindley, Deep scrotal temperature and the effect on it of clothing, air temperature, activity, posture and paraplegia, British Journal of Urology 54 (1982) 49-55.

[66] C. Wang, V. McDonald, A. Leung, L. Superlano, N. Berman, L. Hull, R.S. Swerdloff, Effect of increased scrotal temperature on sperm production in normal men, Fertility and sterility 68 (1997) 334-339.

[67] M. Modaresi, M. Emadi, The effects of rosemary extract on spermatogenesis and sexual hormones of mice under heat stress, Trends Journal of Sciences Research 3 (2018) 69-74.

[68] M. Rao, W. Xia, J. Yang, L.X. Hu, S.F. Hu, H. Lei, Y.Q. Wu, C.H. Zhu, Transient scrotal hyperthermia affects human sperm DNA integrity, sperm apoptosis, and sperm protein expression, Andrology 4 (2016) 1054-1063.

[69] M. Hamerezaee, S.F. Dehghan, F. Golbabaei, A. Fathi, L. Barzegar, N. Heidarnejad, Assessment of semen quality among workers exposed to heat stress: a cross-sectional study in a steel industry, Safety and health at work 9 (2018) 232-235.

[70] Y. Gong, H. Guo, Z. Zhang, H. Zhou, R. Zhao, B. He, Heat stress reduces sperm motility via activation of glycogen synthase kinase-3α and inhibition of mitochondrial protein import, Frontiers in physiology 8 (2017) 718.

[71] S.R. Kopalli, K.-M. Cha, S.-H. Lee, J.-H. Ryu, S.-Y. Hwang, M.-S. Jeong, J.-H. Sung, S.-K. Kim, Pectinase-treated Panax ginseng protects against chronic intermittent heat stress-induced testicular damage by modulating hormonal and spermatogenesis-related molecular expression in rats, Journal of Ginseng Research 41 (2017) 578-588.

[72] J. Yaeram, B. Setchell, S. Maddocks, Effect of heat stress on the fertility of male mice in vivo and in vitro, Reproduction, Fertility and Development 18 (2006) 647-653.

[73] S. Banks, S.A. King, D.S. Irvine, P.T. Saunders, Impact of a mild scrotal heat stress on DNA integrity in murine spermatozoa, Reproduction 129 (2005) 505-514.

[74] R. Bakthisaran, R. Tangirala, C.M. Rao, Small heat shock proteins: role in cellular functions and pathology, Biochimica et Biophysica Acta (BBA)-Proteins and Proteomics 1854 (2015) 291-319.

[75] A.S. Sreedhar, É. Kalmár, P. Csermely, Y.-F. Shen, Hsp90 isoforms: functions, expression and clinical importance, FEBS letters 562 (2004) 11-15.

[76] C. Légaré, M. Thabet, R. Sullivan, Expression of heat shock protein 70 in normal and cryptorchid human excurrent duct, Molecular human reproduction 10 (2004) 197-202.

[77] S.-Y. Huang, M.-F. Tam, Y.-T. Hsu, J.-H. Lin, H.-H. Chen, C.-k. Chuang, M.-Y. Chen, Y.-T. King, W.-C. Lee, Developmental changes of heat-shock proteins in porcine testis by a proteomic analysis, Theriogenology 64 (2005) 1940-1955.

[78] S.K. Moore, C. Kozak, E.A. Robinson, S.J. Ullrich, E. Appella, Murine 86-and 84-kDa heat shock proteins, cDNA sequences, chromosome assignments, and evolutionary origins, Journal of Biological Chemistry 264 (1989) 5343-5351.

[79] S. Ohsako, D. Bunick, Y. Hayashi, Immunocytochemical observation of the 90 KD heat shock protein (HSP90): high expression in primordial and pre-meiotic germ cells of male and female rat gonads, Journal of Histochemistry & Cytochemistry 43 (1995) 67-76.

[80] S.J. Lee, Expression of HSP86 in male germ cells, Molecular and cellular biology 10 (1990) 3239-3242.

[81] Y. Pei, Y. Wu, Y. Qin, Effects of chronic heat stress on the expressions of heat shock proteins 60, 70, 90, A2, and HSC70 in the rabbit testis, Cell Stress and Chaperones 17 (2012) 81-87.

[82] T. Li, W. He, X. Liao, X. Lin, L. Zhang, L. Lu, Y. Guo, Z. Liu, X. Luo, Zinc alleviates the heat stress of primary cultured hepatocytes of broiler embryos via enhancing the antioxidant ability and attenuating the heat shock responses, Animal Nutrition 7 (2021) 621-630.

[83] R.K. Naviaux, Oxidative shielding or oxidative stress?, Journal of Pharmacology and Experimental Therapeutics 342 (2012) 608-618.

[84] A. Agarwal, A. Hamada, S.C. Esteves, Insight into oxidative stress in varicocele-associated male infertility: part 1, Nature Reviews Urology 9 (2012) 678-690.

[85] R.J. Aitken, T.B. Smith, M.S. Jobling, M.A. Baker, G.N. De Iuliis, Oxidative stress and male reproductive health, Asian journal of andrology 16 (2014) 31.

[186] N. Ghasemi, H. Babaei, S. Azizallahi, A. Kheradmand, Effect of long-term administration of zinc after scrotal heating on mice spermatozoa and subsequent offspring quality, Andrologia 41 (2009) 222-228.

[87] R.J. Aitken, S.D. Roman, Antioxidant systems and oxidative stress in the testes, Molecular mechanisms in spermatogenesis (2009) 154-171.

[88] R.D. Moreno, R. Lagos-Cabré, J. Buñay, N. Urzúa, X. Bustamante-Marín, Molecular basis of heat stress damage in mammalian testis, Testis: Anatomy, Physiology and Pathology (2012) 127-155.

[89] A. Delkhosh, H. Shoorei, V. Niazi, M. Delashoub, M.N. Gharamaleki, M. Ahani-Nahayati, Y.K. Dehaghi, S. Raza, M.H. Taheri, M. Mohaqiq, Coenzyme Q10 ameliorates inflammation, oxidative stress, and testicular histopathology in rats exposed to heat stress, Human & Experimental Toxicology 40 (2021) 3-15.

[90] S. Kaur, M. Bansal, Protective role of dietary-supplemented selenium and vitamin E in heat-induced apoptosis and oxidative stress in mice testes, Andrologia 47 (2015) 1109-1119.

[91] A.P.S. Hikim, Y. Lue, C.M. Yamamoto, Y. Vera, S. Rodriguez, P.H. Yen, K. Soeng, C. Wang, R.S. Swerdloff, Key apoptotic pathways for heat-induced programmed germ cell death in the testis, Endocrinology 144 (2003) 3167-3175.

[92] M.O. Hengartner, The biochemistry of apoptosis, Nature 407 (2000) 770-776.

[93] J.M. Adams, S. Cory, The Bcl-2 protein family: arbiters of cell survival, Science 281 (1998) 1322-1326.

[94] J. Lee, J.H. Richburg, S.C. Younkin, K. Boekelheide, The Fas system is a key regulator of germ cell apoptosis in the testis, Endocrinology 138 (1997) 2081-2088.

[95] D. Durairajanayagam, A. Agarwal, C. Ong, Causes, effects and molecular mechanisms of testicular heat stress, Reproductive biomedicine online 30 (2015) 14-27.

[96] M. Zhang, M. Jiang, Y. Bi, H. Zhu, Z. Zhou, J. Sha, Autophagy and apoptosis act as partners to induce germ cell death after heat stress in mice, PloS one 7 (2012) e41412.

[97] A. MORGENTALER, B.C. STAHL, Y. YIN, Testis and temperature: an historical, clinical, and research perspective, Journal of Andrology 20 (1999) 189-195.

[98] J.C. Rockett, F.L. Mapp, J.B. Garges, J.C. Luft, C. Mori, D.J. Dix, Effects of hyperthermia on spermatogenesis, apoptosis, gene expression, and fertility in adult male mice, Biology of reproduction 65 (2001) 229-239.

[99] S.M. Ruwanpura, R.I. McLachlan, S.J. Meachem, Hormonal regulation of male germ cell development, The Journal of endocrinology 205 (2010) 117-131.

[100] H. Lin, S.W. Wang, R.Y. Wang, P.S. Wang, Stimulatory effect of lactate on testosterone production by rat Leydig cells, Journal of cellular biochemistry 83 (2001) 147-154.

[101] D.M. Stocco, StAR protein and the regulation of steroid hormone biosynthesis, Annual review of physiology 63 (2001) 193-213.

[102] Y. Aghazadeh, B.R. Zirkin, V. Papadopoulos, Pharmacological regulation of the cholesterol transport machinery in steroidogenic cells of the testis, Vitamins & Hormones 98 (2015) 189-227.

[103] C. Aktas, M. Kanter, A morphological study on Leydig cells of scrotal hyperthermia applied rats in short-term, Journal of molecular histology 40 (2009) 31-39.

[104] M.B.R. Alves, A.F.C. de Andrade, R.P. de Arruda, L. Batissaco, S.A. Florez-Rodriguez, B.M.M. de Oliveira, M.A. Torres, R. Lançoni, G.M. Ravagnani, R.R. do Prado Filho, Recovery of normal testicular temperature after scrotal heat stress in rams assessed by infrared thermography and its

effects on seminal characteristics and testosterone blood serum concentration, Theriogenology 86 (2016) 795-805. e792.

[105] Z. Li, J. Tian, G. Cui, M. Wang, D. Yu, Effects of local testicular heat treatment on Leydig cell hyperplasia and testosterone biosynthesis in rat testes, Reproduction, Fertility and Development 28 (2016) 1424-1432.

[106] J.-M. Yon, J.S. Kim, C. Lin, S.G. Park, L.W. Gwon, J.-G. Lee, I.-J. Baek, S.-S. Nahm, S.-Y. Nam, Beta-carotene prevents the spermatogenic disorders induced by exogenous scrotal hyperthermia through modulations of oxidative stress, apoptosis, and androgen biosynthesis in mice, Korean Journal of Veterinary Research 59 (2019) 59-67.

[107] A.P. Singh, S. Rajender, CatSper channel, sperm function and male fertility, Reproductive biomedicine online 30 (2015) 28-38.

[108] K.K. Shukla, A.A. Mahdi, S. Rajender, Ion channels in sperm physiology and male fertility and infertility, Journal of andrology 33 (2012) 777-788.

[109] D. Ren, B. Navarro, G. Perez, A.C. Jackson, S. Hsu, Q. Shi, J.L. Tilly, D.E. Clapham, A sperm ion channel required for sperm motility and male fertility, Nature 413 (2001) 603-609.

[110] J.Y. Hwang, N. Mannowetz, Y. Zhang, R.A. Everley, S.P. Gygi, J. Bewersdorf, P.V. Lishko, J.-J. Chung, Dual sensing of physiologic pH and calcium by EFCAB9 regulates sperm motility, Cell 177 (2019) 1480-1494. e1419.

[111] S.G. Brown, S.J. Publicover, C.L. Barratt, S.J. Martins da Silva, Human sperm ion channel (dys) function: implications for fertilization, Human reproduction update 25 (2019) 758-776.

[112] J. Liu, J. Xia, K.-H. Cho, D.E. Clapham, D. Ren, CatSperβ, a novel transmembrane protein in the CatSper channel complex, Journal of Biological Chemistry 282 (2007) 18945-18952.

[113] H. Wang, J. Liu, K.-H. Cho, D. Ren, A novel, single, transmembrane protein CATSPERG is associated with CATSPER1 channel protein, Biology of reproduction 81 (2009) 539-544.

[114] J.-J. Chung, B. Navarro, G. Krapivinsky, L. Krapivinsky, D.E. Clapham, A novel gene required for male fertility and functional CATSPER channel formation in spermatozoa, Nature communications 2 (2011) 1-12.

[115] K.-W. Cheon, Y.-J. Choi, H.-K. Byun, J.-Y. Hong, H.-K. Choi, J.-T. Seo, Expression of sperm-specific cation channel CatSper in human spermatozoa, Korean Journal of Urology (2004) 365-372.

[116] A. Lobley, V. Pierron, L. Reynolds, L. Allen, D. Michalovich, Identification of human and mouse CatSper3 and CatSper4 genes: characterisation of a common interaction domain and evidence for expression in testis, Reproductive biology and endocrinology 1 (2003) 1-15.

[117] B. Navarro, Y. Kirichok, J.-J. Chung, D.E. Clapham, Ion channels that control fertility in mammalian spermatozoa, The International journal of developmental biology 52 (2008) 607.

[118] H. Qi, M.M. Moran, B. Navarro, J.A. Chong, G. Krapivinsky, L. Krapivinsky, Y. Kirichok, I.S. Ramsey, T.A. Quill, D.E. Clapham, All four CatSper ion channel proteins are required for male fertility and sperm cell hyperactivated motility, Proceedings of the National Academy of Sciences 104 (2007) 1219-1223.

[119] T.A. Quill, D. Ren, D.E. Clapham, D.L. Garbers, A voltage-gated ion channel expressed specifically in spermatozoa, Proceedings of the National Academy of Sciences 98 (2001) 12527-12531.

[120] K. Schuh, E.J. Cartwright, E. Jankevics, K. Bundschu, J. Liebermann, J.C. Williams, A.L. Armesilla, M. Emerson, D. Oceandy, K.-P. Knobeloch, Plasma membrane Ca2+ ATPase 4 is required for sperm motility and male fertility, Journal of Biological Chemistry 279 (2004) 28220-28226.

[121] Z. Krasznai, Z.T. Krasznai, M. Morisawa, Z.K. Bazsáné, Z. Hernádi, Z. Fazekas, L. Trón, K. Goda, T. Márián, Role of the Na+/Ca2+ exchanger

in calcium homeostasis and human sperm motility regulation, Cell motility and the cytoskeleton 63 (2006) 66-76.

[122] H.M. Florman, M.K. Jungnickel, K.A. Sutton, Regulating the acrosome reaction, International Journal of Developmental Biology 52 (2004) 503-510.

[123] C.M. Santi, P. Martínez-López, J.L. de la Vega-Beltrán, A. Butler, A. Alisio, A. Darszon, L. Salkoff, The SLO3 sperm-specific potassium channel plays a vital role in male fertility, FEBS letters 584 (2010) 1041-1046.

[124] P.E. Visconti, D. Krapf, J.L. De La Vega-beltrán, J.J. Acevedo, A. Darszon, Ion channels, phosphorylation and mammalian sperm capacitation, Asian journal of andrology 13 (2011) 395.

[125] C.L. Barratt, S.J. Publicover, Sperm are promiscuous and CatSper is to blame…, The EMBO Journal 31 (2012) 1624-1626.

[126] B. Marquez, G. Ignotz, S.S. Suarez, Contributions of extracellular and intracellular Ca2+ to regulation of sperm motility: release of intracellular stores can hyperactivate CatSper1 and CatSper2 null sperm, Developmental biology 303 (2007) 214-221.

[127] J. Jin, N. Jin, H. Zheng, S. Ro, D. Tafolla, K.M. Sanders, W. Yan, Catsper3 and Catsper4 are essential for sperm hyperactivated motility and male fertility in the mouse, Biology of reproduction 77 (2007) 37-44.

[128] J.C. Kirkman-Brown, D.J. Smith, Sperm motility: is viscosity fundamental to progress?, MHR: Basic science of reproductive medicine 17 (2011) 539-544.

[129] X.-h. Sun, Y.-y. Zhu, L. Wang, H.-l. Liu, Y. Ling, Z.-l. Li, L.-b. Sun, The Catsper channel and its roles in male fertility: a systematic review, Reproductive Biology and Endocrinology 15 (2017) 1-12.

[130] C. Brenker, N. Goodwin, I. Weyand, N.D. Kashikar, M. Naruse, M. Krähling, A. Müller, U.B. Kaupp, T. Strünker, The CatSper channel: a polymodal chemosensor in human sperm, The EMBO journal 31 (2012) 1654-1665.

[131] Y. Kirichok, B. Navarro, D.E. Clapham, Whole-cell patch-clamp measurements of spermatozoa reveal an alkaline-activated Ca2+ channel, Nature 439 (2006) 737-740.

[132] J. Mahsa Askari, M. Mansoureh, M. Zohreh, A. Masoud, M. Seyed Javad, B. Hosein, Evaluating the effects of Escanbil [Calligonum] extract on the expression level of Catsper gene variants and sperm motility in aging male mice, (2014).

[133] J. Rezaian, M. Movahedin, S.J. Mowla, CatSper genes expression, semen characteristics and histology of testes in the contusive spinal cord-injured mice model, Spinal Cord 47 (2009) 76-81.

[134] M. Amini, P. Shirinbayan, B. Behnam, M. Roghani, A. Farhoudian, M. Joghataei, M. Koruji, Correlation between expression of CatSper family and sperm profiles in the adult mouse testis following I ranian Kerack abuse, Andrology 2 (2014) 386-393.

[135] A.E. Carlson, T.A. Quill, R.E. Westenbroek, S.M. Schuh, B. Hille, D.F. Babcock, Identical phenotypes of CatSper1 and CatSper2 null sperm, Journal of Biological Chemistry 280 (2005) 32238-32244.

[136] Y. Matsumura, H. Maeda, A new concept for macromolecular therapeutics in cancer chemotherapy: mechanism of tumoritropic accumulation of proteins and the antitumor agent smancs, Cancer research 46 (1986) 6387-6392.

[137] H. Maeda, Toward a full understanding of the EPR effect in primary and metastatic tumors as well as issues related to its heterogeneity, Advanced drug delivery reviews 91 (2015) 3-6.

[138] Y. Nakamura, A. Mochida, P.L. Choyke, H. Kobayashi, Nanodrug delivery: is the enhanced permeability and retention effect sufficient for curing cancer?, Bioconjugate chemistry 27 (2016) 2225-2238.

[139] D. Rosenblum, N. Joshi, W. Tao, J.M. Karp, D. Peer, Progress and challenges towards targeted delivery of cancer therapeutics, Nature communications 9 (2018) 1-12.

[140] L. Duan, L. Yang, J. Jin, F. Yang, D. Liu, K. Hu, Q. Wang, Y. Yue, N. Gu, Micro/nano-bubble-assisted ultrasound to enhance the EPR effect and potential theranostic applications, Theranostics 10 (2020) 462.

[141] W. Islam, J. Fang, T. Imamura, T. Etrych, V. Subr, K. Ulbrich, H. Maeda, Augmentation of the enhanced permeability and retention effect with nitric oxide–generating agents improves the therapeutic effects of nanomedicines, Molecular cancer therapeutics 17 (2018) 2643-2653.

[142] R. Kinoshita, Y. Ishima, V.T. Chuang, H. Nakamura, J. Fang, H. Watanabe, T. Shimizu, K. Okuhira, T. Ishida, H. Maeda, Improved anticancer effects of albumin-bound paclitaxel nanoparticle via augmentation of EPR effect and albumin-protein interactions using S-nitrosated human serum albumin dimer, Biomaterials 140 (2017) 162-169.

[143] A. Nagamitsu, K. Greish, H. Maeda, Elevating blood pressure as a strategy to increase tumor-targeted delivery of macromolecular drug SMANCS: cases of advanced solid tumors, Japanese journal of clinical oncology 39 (2009) 756-766.

[144] Y. Tahara, T. Yoshikawa, H. Sato, Y. Mori, M.H. Zahangir, A. Kishimura, T. Mori, Y. Katayama, Encapsulation of a nitric oxide donor into a liposome to boost the enhanced permeation and retention (EPR) effect, MedChemComm 8 (2017) 415-421.

[145] W.L. Monsky, D. Fukumura, T. Gohongi, M. Ancukiewcz, H.A. Weich, V.P. Torchilin, F. Yuan, R.K. Jain, Augmentation of transvascular transport of macromolecules and nanoparticles in tumors using vascular endothelial growth factor, Cancer Research 59 (1999) 4129-4135.

[146] M. Magzoub, S. Jin, A. Verkman, Enhanced macromolecule diffusion deep in tumors after enzymatic digestion of extracellular matrix collagen and its associated proteoglycan decorin, The FASEB Journal 22 (2008) 276-284.

[147] H. Kobayashi, K. Reijnders, S. English, A.T. Yordanov, D.E. Milenic, A.L. Sowers, D. Citrin, M.C. Krishna, T.A. Waldmann, J.B. Mitchell, Application of a macromolecular contrast agent for detection of alterations

of tumor vessel permeability induced by radiation, Clinical cancer research 10 (2004) 7712-7720.

[148] L. Li, T.L. ten Hagen, M. Bolkestein, A. Gasselhuber, J. Yatvin, G.C. van Rhoon, A.M. Eggermont, D. Haemmerich, G.A. Koning, Improved intratumoral nanoparticle extravasation and penetration by mild hyperthermia, Journal of Controlled Release 167 (2013) 130-137.

[149] A. Dhaliwal, G. Zheng, Improving accessibility of EPR-insensitive tumor phenotypes using EPR-adaptive strategies: Designing a new perspective in nanomedicine delivery, Theranostics 9 (2019) 8091.

[150] J. Fang, W. Islam, H. Maeda, Exploiting the dynamics of the EPR effect and strategies to improve the therapeutic effects of nanomedicines by using EPR effect enhancers, Advanced drug delivery reviews 157 (2020) 142-160.

[151] M. Hasan, A. Nishimoto, T. Ohgita, S. Hama, H. Kashida, H. Asanuma, K. Kogure, Faint electric treatment-induced rapid and efficient delivery of extraneous hydrophilic molecules into the cytoplasm, Journal of Controlled Release 228 (2016) 20-25.

[152] M. Hasan, A. Khatun, T. Fukuta, K. Kogure, Noninvasive transdermal delivery of liposomes by weak electric current, Advanced Drug Delivery Reviews 154 (2020) 227-235.

[153] K. Kajimoto, M. Yamamoto, M. Watanabe, K. Kigasawa, K. Kanamura, H. Harashima, K. Kogure, Noninvasive and persistent transfollicular drug delivery system using a combination of liposomes and iontophoresis, International journal of pharmaceutics 403 (2011) 57-65.

[154] T. Torao, M. Mimura, Y. Oshima, K. Fujikawa, M. Hasan, T. Shimokawa, N. Yamazaki, H. Ando, T. Ishida, T. Fukuta, Characteristics of unique endocytosis induced by weak current for cytoplasmic drug delivery, International Journal of Pharmaceutics 576 (2020) 119010.

[155] M. Hasan, S. Hama, K. Kogure, Low electric treatment activates Rho GTPase via heat shock protein 90 and protein kinase C for intracellular delivery of siRNA, Scientific reports 9 (2019) 1-12.

[156] T. Fukuta, S. Yoshimi, K. Kogure, Leukocyte-Mimetic Liposomes Penetrate Into Tumor Spheroids and Suppress Spheroid Growth by Encapsulated Doxorubicin, Journal of Pharmaceutical Sciences 110 (2021) 1701-1709.

[157] M. Toyoda, S. Hama, Y. Ikeda, Y. Nagasaki, K. Kogure, Anti-cancer vaccination by transdermal delivery of antigen peptide-loaded nanogels via iontophoresis, International Journal of Pharmaceutics 483 (2015) 110-114.

[158] V. A. Smits, R. H. Medema, Checking out the G2/M transition. Biochimica et Biophysica Acta (BBA)-Gene Structure and Expression, 1519 (1-2) (2001) 1-12.

[159] I. Epifantseva, R.M. Shaw, Intracellular trafficking pathways of Cx43 gap junction channels, Biochimica et Biophysica Acta (BBA)-Biomembranes 1860 (2018) 40-47.

[160] A.E. Pereda, S. Curti, G. Hoge, R. Cachope, C.E. Flores, J.E. Rash, Gap junction-mediated electrical transmission: regulatory mechanisms and plasticity, Biochimica et Biophysica Acta (BBA)-Biomembranes 1828 (2013) 134-146.

[161] M.W. Bobbie, S. Roy, K. Trudeau, S.J. Munger, A.M. Simon, S. Roy, Reduced connexin 43 expression and its effect on the development of vascular lesions in retinas of diabetic mice, Investigative ophthalmology & visual science 51 (2010) 3758-3763.

[162] R. Fernandes, H. Girao, P. Pereira, High glucose down-regulates intercellular communication in retinal endothelial cells by enhancing degradation of connexin 43 by a proteasome-dependent mechanism, Journal of Biological Chemistry 279 (2004) 27219-27224.

[163] J.L. Solan, P.D. Lampe, Specific Cx43 phosphorylation events regulate gap junction turnover in vivo, FEBS letters 588 (2014) 1423-1429.

[164] W. Liu, Y. Cui, J. Wei, J. Sun, L. Zheng, J. Xie, Gap junction-mediated cell-to-cell communication in oral development and oral diseases: a concise review of research progress, International journal of oral science 12 (2020) 1-9.

[165] M.-E. Bonnet, J.-B. Gossart, E. Benoit, M. Messmer, O. Zounib, V. Moreau, J.-P. Behr, N. Lenne-Samuel, V. Kedinger, A. Meulle, Systemic delivery of sticky siRNAs targeting the cell cycle for lung tumor metastasis inhibition, Journal of Controlled Release 170 (2013) 183-190.

[166] V. Kedinger, A. Meulle, O. Zounib, M.-E. Bonnet, J.-B. Gossart, E. Benoit, M. Messmer, P. Shankaranarayanan, J.-P. Behr, P. Erbacher, Sticky siRNAs targeting survivin and cyclin B1 exert an antitumoral effect on melanoma subcutaneous xenografts and lung metastases, BMc cancer 13 (2013) 1-11.

[167] Y. Song, C. Zhao, L. Dong, M. Fu, L. Xue, Z. Huang, T. Tong, Z. Zhou, A. Chen, Z. Yang, Overexpression of cyclin B1 in human esophageal squamous cell carcinoma cells induces tumor cell invasive growth and metastasis, Carcinogenesis 29 (2008) 307-315.

[168] Y. Fang, H. Yu, X. Liang, J. Xu, X. Cai, Chk1-induced CCNB1 overexpression promotes cell proliferation and tumor growth in human colorectal cancer, Cancer biology & therapy 15 (2014) 1268-1279.

[169] I.D. Sharlip, J.P. Jarow, A.M. Belker, L.I. Lipshultz, M. Sigman, A.J. Thomas, P.N. Schlegel, S.S. Howards, A. Nehra, M.D. Damewood, Best practice policies for male infertility, Fertility and sterility 77 (2002) 873-882.

[170] I. Briceag, A. Costache, V. Purcarea, R. Cergan, M. Dumitru, I. Briceag, M. Sajin, A. Ispas, Fallopian tubes–literature review of anatomy and etiology in female infertility, Journal of medicine and life 8 (2015) 129.

[171] N. Kumar, A.K. Singh, Trends of male factor infertility, an important cause of infertility: A review of literature, Journal of human reproductive sciences 8 (2015) 191.

[172] X. Qi, K. Wang, G. Zhou, Z. Xu, J. Yu, W. Zhang, The role of testicular artery in laparoscopic varicocelectomy: a systematic review and meta-analysis, International Urology and Nephrology 48 (2016) 955-965.

[173] R. Harrison, Abdoimino-testicular temperature gradients, J. Physiol. 107 (1948) 48-49.

[174] C. Lin, D.-G. Shin, S.G. Park, S.B. Chu, L.W. Gwon, J.-G. Lee, J.-M. Yon, I.-J. Baek, S.-Y. Nam, Curcumin dose-dependently improves spermatogenic disorders induced by scrotal heat stress in mice, Food & function 6 (2015) 3770-3777.

[175] S. Shadmehr, S.R.F. Tabatabaei, S. Hosseinifar, M.R. Tabandeh, A. Amiri, Attenuation of heat stress-induced spermatogenesis complications by betaine in mice, Theriogenology 106 (2018) 117-126.

[176] Y. Barazani, B.F. Katz, H.M. Nagler, D.S. Stember, Lifestyle, environment, and male reproductive health, Urologic Clinics 41 (2014) 55-66.

[177] B. Kim, K. Park, K. Rhee, Heat stress response of male germ cells, Cellular and Molecular Life Sciences 70 (2013) 2623-2636.

[178] N. Aydilek, O. Varisli, A. Kocyigit, A. Taskin, M. Kaya, Effect of dietary restriction on sperm characteristic and oxidative status on testicular tissue in young rats exposed to long-term heat stress, Andrologia 47 (2015) 1055-1061.

[179] A. Rasooli, M.T. Jalali, M. Nouri, B. Mohammadian, F. Barati, Effects of chronic heat stress on testicular structures, serum testosterone and cortisol concentrations in developing lambs, Animal reproduction science 117 (2010) 55-59.

[180] P. Wang, Y. Li, X.-c. Hu, X.-L. Cai, L.-P. Hou, Y.-F. Wang, J.-H. Hu, Q.-W. Li, L.-J. Suo, Z.-G. Fan, Cryoprotective effects of low-density lipoproteins, trehalose and soybean lecithin on murine spermatogonial stem cells, Zygote 22 (2014) 158-163.

[181] A. Darszon, T. Nishigaki, C. Beltran, C.L. Treviño, Calcium channels in the development, maturation, and function of spermatozoa, Physiological reviews 91 (2011) 1305-1355.

[182] P.V. Lishko, Y. Kirichok, D. Ren, B. Navarro, J.-J. Chung, D.E. Clapham, The control of male fertility by spermatozoan ion channels, Annual review of physiology 74 (2012) 453-475.

[183] J.-J. Chung, K. Miki, D. Kim, S.-H. Shim, H.F. Shi, J.Y. Hwang, X. Cai, Y. Iseri, X. Zhuang, D.E. Clapham, CatSperζ regulates the structural continuity of sperm Ca2+ signaling domains and is required for normal fertility, Elife 6 (2017) e23082.

[184] J.-L. Jin, A.M. O'Doherty, S. Wang, H. Zheng, K.M. Sanders, W. Yan, Catsper3 and catsper4 encode two cation channel-like proteins exclusively expressed in the testis, Biology of reproduction 73 (2005) 1235-1242.

[185] T.A. Quill, S.A. Sugden, K.L. Rossi, L.K. Doolittle, R.E. Hammer, D.L. Garbers, Hyperactivated sperm motility driven by CatSper2 is required for fertilization, Proceedings of the National Academy of Sciences 100 (2003) 14869-14874.

[186] H.-F. Wang, M. Liu, N. Li, T. Luo, L.-P. Zheng, X.-H. Zeng, Bisphenol a impairs mature sperm functions by a CatSper-relevant mechanism, Toxicological Sciences 152 (2016) 145-154.

[187] H.-F. Wang, M. Chang, T.-T. Peng, Y. Yang, N. Li, T. Luo, Y.-M. Cheng, M.-Z. Zhou, X.-H. Zeng, L.-P. Zheng, Exposure to cadmium impairs sperm functions by reducing CatSper in mice, Cellular physiology and biochemistry 42 (2017) 44-54.

[188] A. Srivastav, B. Changkija, K. Sharan, G.K. Nagar, F.W. Bansode, Influence of antifertility agents Dutasteride and Nifedipine on CatSper gene level in epididymis during sperm maturation in BALB/c mice, Reproduction 155 (2018) 347-359.

[189] Z. Allaeian Jahromi, M.H. Meshkibaf, M. Naghdi, A. Vahdati, Z. Makoolati, Methamphetamine Downregulates the Sperm-Specific Calcium Channels Involved in Sperm Motility in Rats, ACS omega 7 (2022) 5190-5196.

[190] M.Z. Soleimani, F.J. Mashayekhi, M.M. Hasanzade, M. Baazm, Alteration in CatSper1 and 2 genes expression, sperm parameters and testis histology in varicocelized rats, International Journal of Reproductive Biomedicine 16 (2018) 183.

[191] E. Hafez, Rabbits, Reproduction and breeding techniques for laboratory animals (1970) 273-315.

[192] V.L. Slott, J.D. Suarez, S.D. Perreault, Rat sperm motility analysis: methodologic considerations, Reproductive Toxicology 5 (1991) 449-458.

[193] G. Robb, R. Amann, G. Killian, Daily sperm production and epididymal sperm reserves of pubertal and adult rats, Reproduction 54 (1978) 103-107.

[194] R. Filler, Methods for evaluation of rat epididymal sperm morphology, Methods in Toxicology 3 (1993) 334-343.

[195] J. Hand, H. Walker, S. Hornsey, S. Field, Effects of hyperthermia on the mouse testis and its response to X-rays, as assayed by weight loss, International Journal of Radiation Biology and Related Studies in Physics, Chemistry and Medicine 35 (1979) 521-528.

[196] B.L. SAILER, L.J. SARKAR, J.A. BJORDAHL, L.K. JOST, D.P. EVENSON, Effects of heat stress on mouse testicular cells and sperm chromatin structure, Journal of Andrology 18 (1997) 294-301.

[197] M. Nicolino, M. Forest, La puberté, La reproduction chez les mammifères et l'homme. Volume 29 (2001).

[198] A. Gasinska, S. HILLI, The effect oi hyperthermia on the mouse testis, Neoplasma 37 (1990) 357.

[199] M. Kobeasyab, A. El-Naggarac, A. Abdallahd, A novel methods for protective role against reproductive toxicity of carbofuren in male rats using palm pollen grains and vanadyl (II) folate as a new compound, Journal of Chemical and Pharmaceutical Research 7 (2015) 1142-1148.

[200] N. Mahdivand, G. Najafi, V. Nejati, A. Shalizar-Jalali, F. Rahmani, Royal jelly protects male rats from heat stress-induced reproductive failure, Andrologia 51 (2019) e13213.

[201] J. Kastelic, R. Wilde, G. Rizzoto, J. Thundathil, Hyperthermia and not hypoxia may reduce sperm motility and morphology following testicular hyperthermia, Veterinární medicína 62 (2017) 437-442.

[202] A. Agarwal, D. Durairajanayagam, J. Halabi, J. Peng, M. Vazquez-Levin, Proteomics, oxidative stress and male infertility, Reproductive biomedicine online 29 (2014) 32-58.

[203] P. Nikpoor, S.J. Mowla, M. Movahedin, S.A.M. Ziaee, T. Tiraihi, CatSper gene expression in postnatal development of mouse testis and in subfertile men with deficient sperm motility, Human reproduction 19 (2004) 124-128.

[204] Z.A. Jahromi, M.H. Meshkibaf, M. Naghdi, A. Vahdati, Z. Makoolati, Methamphetamine Downregulates the Sperm-Specific Calcium Channels Involved in Sperm Motility in Rats, ACS omega 7 (2022) 5190.

[205] Z.-R. Jin, D. Fang, B.-H. Liu, J. Cai, W.-H. Tang, H. Jiang, G.-G. Xing, Roles of CatSper channels in the pathogenesis of asthenozoospermia and the therapeutic effects of acupuncture-like treatment on asthenozoospermia, Theranostics 11 (2021) 2822.

[206] K. Ho, C.A. Wolff, S.S. Suarez, CatSper-null mutant spermatozoa are unable to ascend beyond the oviductal reservoir, Reproduction, Fertility and Development 21 (2009) 345-350.

[207] K. Shiraishi, H. Takihara, H. Matsuyama, Elevated scrotal temperature, but not varicocele grade, reflects testicular oxidative stress-mediated apoptosis, World journal of urology 28 (2010) 359-364.

[208] Y. Li, Y. Huang, Y. Piao, K. Nagaoka, G. Watanabe, K. Taya, C. Li, Protective effects of nuclear factor erythroid 2-related factor 2 on whole body heat stress-induced oxidative damage in the mouse testis, Reproductive Biology and Endocrinology 11 (2013) 1-10.